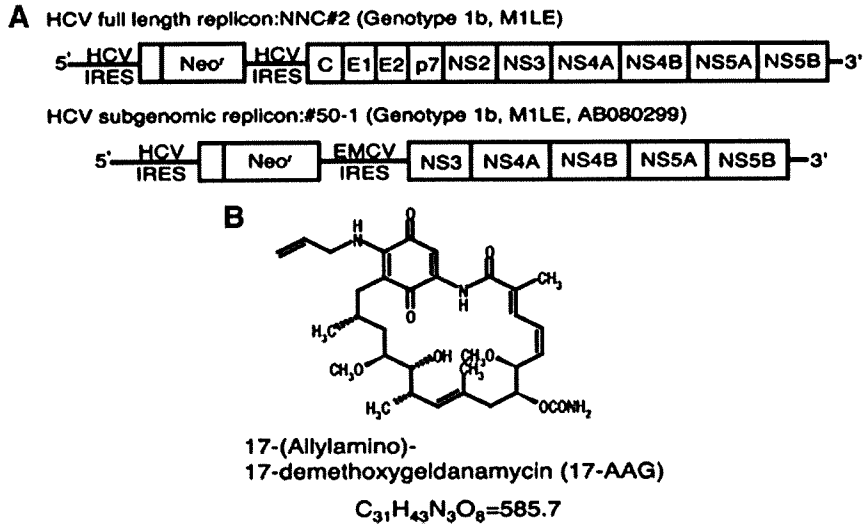

FIGURE 1. **Schematic representation of HCV replicon and structure of 17-AAG.** *A*, structure of the HCV replicon RNAs, comprising the HCV 5′-untranslated region, including the HCV internal ribosome entry site (*IRES*), the neomycin phosphotransferase gene (*Neo'*), the encephalomyocarditis virus (*EMCV*) IRES or HCV IRES, and the coding region for HCV proteins NS3 to NS5B (in the HCV subgenomic replicon) or core to NS5B (in the HCV full-length replicon). *B*, structures of the Hsp90 inhibitor, 17-AAG.

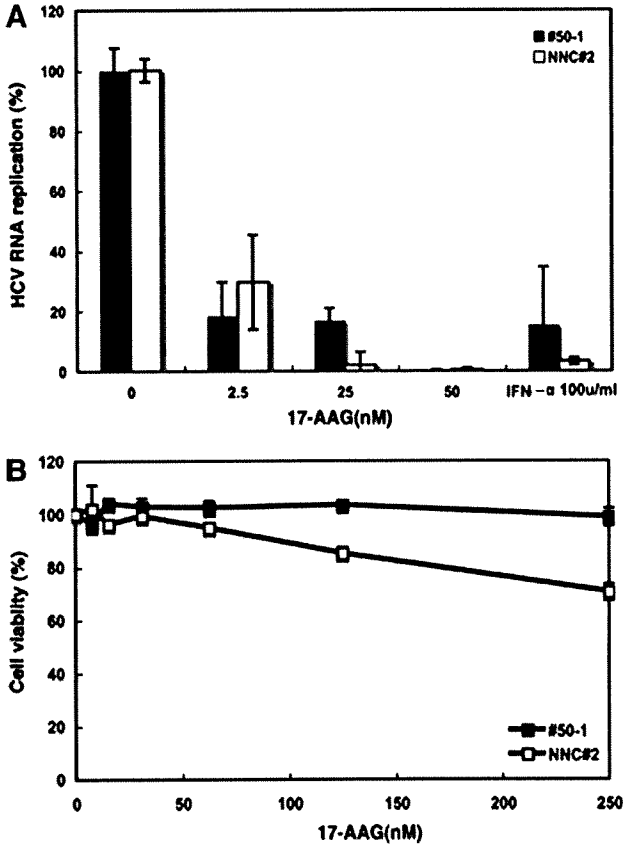

FIGURE 2. **Hsp90 inhibits HCV RNA replication in HCV replicon cells.** *A*, inhibition of HCV replication by 17-AAG in NNC#2 (*white squares*) and #50-1 cells (*black squares*) measured by real time reverse transcription-PCR after 72 h. Interferon-α was used as a positive control. The data are means ± S.D. from triplicate experiments. *B*, cytotoxic effects of 17-AAG in NNC#2 (*white squares*) and #50-1 (*black squares*), shown as the percentage reduction in viable cell numbers in an [3-(4,5-dimethylthiazol-2-yl)-5-(3-carboxymethoxyphenyl)-2-(4-sulfophenyl)-2H-tetrazolium (inner salt)] assay. The data are means ± S.D. from triplicate experiments.

the Hsp90 inhibitor, 17-AAG, suppressed HCV RNA replication, and that the only HCV protein degraded in these cells was NS3, we suggest a crucial role for Hsp90-NS3 protein complexes in the HCV life cycle.

EXPERIMENTAL PROCEDURES

Cell Culture and Reagents—The HCV replicon cell lines #50-1 (NN/1b/SG) (40), which carries a subgenomic replicon, and NNC#2 (NN/1b/FL) (41), which carries a full genome replicon, were cultured in Dulbecco's modified Eagle's medium supplemented with 10% fetal bovine serum, nonessential amino acids, L-glutamine, penicillin/streptomycin, and 300–1,000 μg/ml G418 (Invitrogen) at 37 °C in 5% CO_2. The human embryonic kidney-derived cell line 293T was grown in Dulbecco's modified Eagle's medium supplemented with 10% fetal bovine serum, 100 units/ml penicillin, and 100 μg/ml streptomycin. 17-AAG was purchased from Sigma.

Measuring HCV RNA by Real Time PCR—HCV replicon cells were seeded at 1.5×10^5 cells in 24-well plates and cultured for 72 h. Total RNA was then isolated using TRIzol (Invitrogen) according to the manufacturer's instructions. HCV RNA was quantified by real time reverse transcription-PCR using an ABI 7700 sequence detector (PerkinElmer Life Sciences) and the following primers and TaqMan probes located in the 5′-untranslated region: forward primer (nucleotides 130–146), 5′-CGGGAGAGCCATAGTGG-3′; reverse primer (nucleotides 272–290), 5′-AGTACCACAAGGCCTTTCG-3′; and TaqMan probe (nucleotides 148–168), 5′-CTGCGGAACCGGTGAGTACAC-3′ (all purchased from Applied Biosystems). The probe sequence was labeled with the reporter dye, 6-carboxyflurorescein, at the 5′-end and with the quencher dye TAMRA at the 3′-end (42).

Western Blotting and Immunoprecipitation Analyses—Cells were lysed in 1× CAT enzyme-linked immunosorbent assay buffer (Roche Applied Sciences). Cell lysates were separated by SDS-PAGE and transferred to nitrocellulose membranes, and these were blocked with 5% skimmed milk. The primary antibodies used were monoclonal or polyclonal antibody against FLAG-M5 (Sigma), Hsp70 (Sigma), Hsp90 (Cell Signaling Technologies, Danvers, MA), Hsp90α (Calbiochem), Hsp90β (Calbiochem), and Hsf-1 (Calbiochem). Core, NS4A, and NS4B were a gift from Dr. M. Kohara (Tokyo Metropolitan Institute of Medical Science). E1, E2, NS3, NS5A, and NS5B were a gift from Prof. Y. Matsuura (Osaka University, Japan). Immunoprecipitation from cell lysates was carried out using anti-FLAG M5 antibody (Sigma) and the Protein G immunoprecipitation kit (Sigma), according to the manufacturer's instructions, and the immunoprecipitates were analyzed by Western blotting.

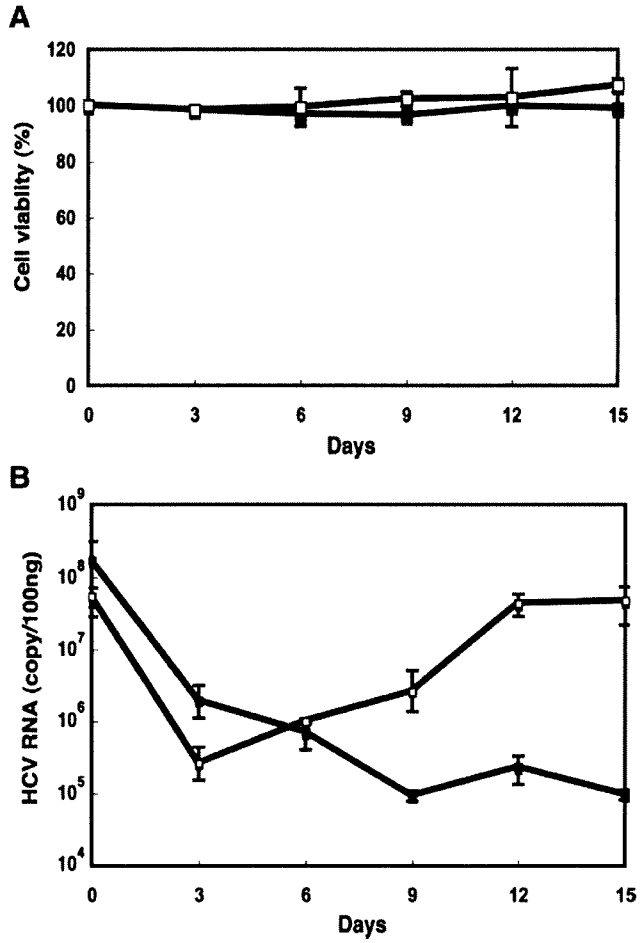

FIGURE 3. **Long term inhibition of HCV replication in NNC#2 cells.** *A*, cytotoxic effect of 17-AAG in NNC#2 cells, shown as the percentage reduction of viable cell numbers assessed by trypan blue staining. NNC#2 cells were treated with 50 nM 17-AAG on day 0 only (*white squares*) or at 3-day intervals for 15 days (*black squares*). The data are means ± S.D. from triplicate experiments. *B*, measurement of HCV replication by real time reverse transcription-PCR. Inhibition of HCV RNA replication in NNC#2 cells treated with 50 nM 17-AAG on day 0 only (*white squares*) or at 3-day intervals for 15 days (*black squares*). *Day 0*, mock. The data are means ± S.D. from triplicate experiments.

[3-(4,5-dimethylthiazol-2-yl)-5-(3-carboxymethoxyphenyl)-2-(4-sulfophenyl)-2H-tetrazolium, inner salt Assay—HCV replicon cells were seeded in 96-well plates at 3×10^4 cells/well in a final culture volume of 100 μl for 72 h before the addition of increasing concentrations of 17-AAG. After incubation for 3 days, viable cell numbers were determined using the Celltiter 96 Aqueous nonradioactive cell proliferation assay (Promega Corp., Madison, WI). The value of the background absorbance at 490 nm (A_{490}) of wells without cells was subtracted. The percentages of viable cells were then calculated using the formula, (A_{490} of 17-AAG-treated sample/A_{490} of untreated cells) × 100.

Plasmids and Transfection—The pFLAG-CMV-NS3 vector was constructed by subcloning a DNA fragment encoding full-length NS3, Δhelicase, Δprotease, ΔPH 1, ΔPH 2, and ΔH 1 into the EcoRI and XbaI sites of the pFLAG-CMV™-2 expression vector (Sigma), so that the amino-terminal FLAG epitope was fused in frame with NS3. The core expression vector was a gift

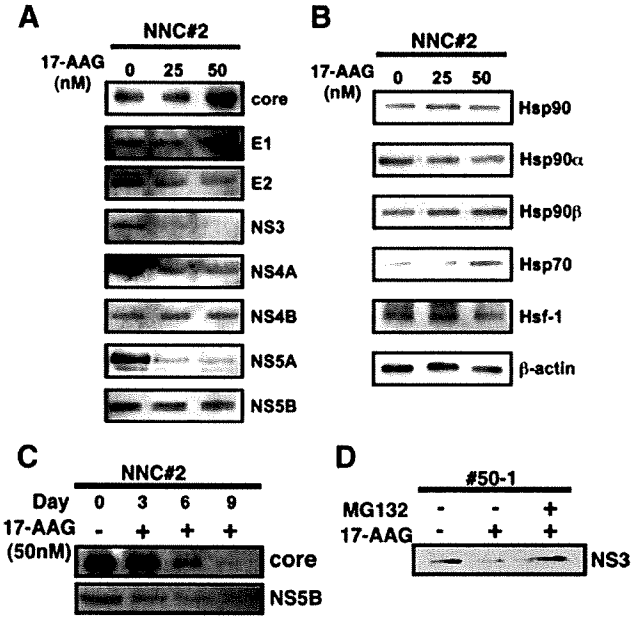

FIGURE 4. **Effect of 17-AAG on HCV NS3 protein levels.** *A*, Western blot analysis of HCV protein expression in NNC#2 or #50-1 cells treated with 17-AAG. NNC#2 or #50-1 cells were treated with 25 and 50 nM 17-AAG for 3 days. Cell lysates were separated by SDS-PAGE, immunoblotted, and probed with antibodies specific for HCV core, E1, E2, NS3, NS4A, NS4B, NS5A, and NS5B. *B*, Western blot analysis of Hsp90, Hsp70, and other chaperone expression in NNC#2 cells treated with 17-AAG (25 and 50 nM, as indicated) for 3 days. *C*, expression of HCV core and NS5B protein in cells treated with 50 nM 17-AAG for 9 days. *D*, effect of 50 nM 17-AAG on NS3 expression in #50-1 cells simultaneously treated with 100 nM MG132.

from Dr. M. Kohara. The vector was transfected into 293T cells using the FuGENE 6 transfection reagent (Roche Applied Science) according to the manufacturer's instructions.

RESULTS

Hsp90 Inhibitor 17-AAG Suppresses HCV RNA Replication—To investigate the effect of 17-AAG on HCV replication, cells containing a full HCV genome replicon (NNC#2) or a subgenomic replicon (#50-1) were treated with 17-AAG (Fig. 1, *A* and *B*). Both of the HCV replicon cell lines were treated for 72 h with different concentrations of 17-AAG or with DMSO as a control. In cells treated with 50 nM 17-AAG, HCV RNA replication was suppressed by 99% in both of the HCV replicon cell lines, and the inhibition of RNA replication occurred in a dose-dependent manner (Fig. 2*A*). The half-maximal inhibitory concentration (IC_{50}) values of 17-AAG for HCV replication were 0.3 nM in NNC#2 cells and 0.1 nM in #50-1 cells. Furthermore, we used a tetrazolium-based [3-(4,5-dimethylthiazol-2-yl)-5-(3-carboxymethoxyphenyl)-2-(4-sulfophenyl)-2H-tetrazolium, inner salt assay to determine the viability of NNC#2 and #50-1 cells in the presence of 17-AAG. 17-AAG showed no toxicity to NNC#2 and #50-1 cells at 50 nM, (Fig. 2*B*). These results suggested that 17-AAG had a greater inhibitory effect on HCV RNA replication than 100 units/ml interferon-α.

Long Term Suppression of HCV RNA Replication—We next examined the effect of 17-AAG on HCV replication over time. When NNC#2 cells were cultured with 50 nM 17-AAG only on day 0 (*white squares*), the level of HCV RNA was reduced by 2 log on day 3 but had increased to control levels by day 12 (Fig.

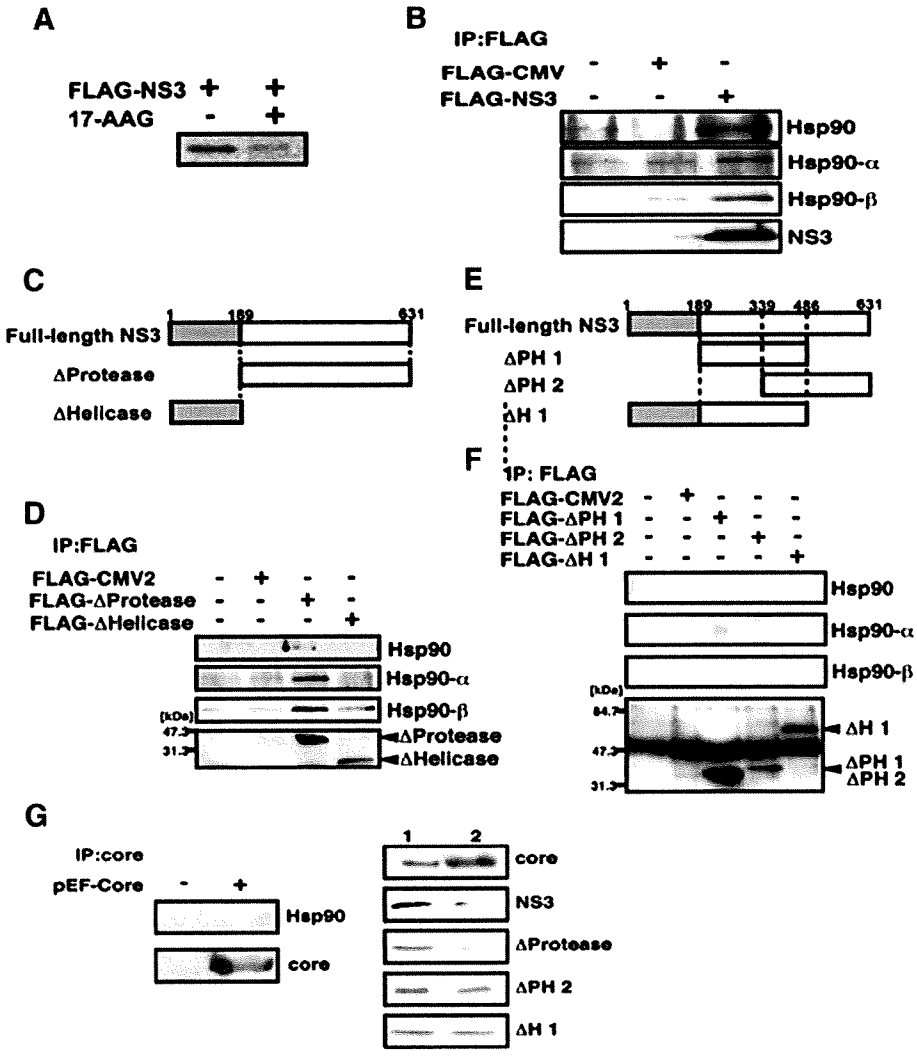

FIGURE 5. **Hsp90 regulates HCV NS3 protein stability.** *A*, Western blot showing the inhibition of NS3 protein expression in 293T cells caused by 17-AAG. Cells were transfected with pFLAG-NS3 in the presence of 250 nM 17-AAG for 48 h. *B*, FLAG-NS3 was expressed in 293T cells and immunoprecipitated (*IP*) from cell lysates with anti-FLAG antibody. Proteins immunoprecipitated were analyzed by Western blotting using anti-Hsp90, anti-Hsp90α, anti-Hsp90β, and anti-FLAG antibodies. The data shown in each *panel* are representative of three independent experiments. *FLAG-CMV*, empty plasmid vector. *C*, schematic representations of HCV NS3 protein and its deletion mutants. *D*, FLAG-NS3, FLAG-Δprotease, and FLAG-Δhelicase were expressed in 293T cells and immunoprecipitated from cell lysates with anti-FLAG antibody. Proteins immunoprecipitated with anti-Hsp90, Hsp90α, Hsp90β, and FLAG antibodies were analyzed by Western blotting. The data shown in each panel are representative of three independent experiments. *E*, schematic representations of HCV NS3 protein and further deletion mutants. *F*, FLAG-ΔPH 1, FLAG-ΔPH 2, and FLAG-ΔH 1 were expressed in 293T cells and immunoprecipitated from cell lysates with anti-FLAG antibody. Proteins immunoprecipitated with anti-Hsp90, Hsp90α, Hsp90β, and FLAG antibodies were analyzed by Western blotting. The data shown in each panel are representative of three independent experiments. *G*, FLAG-NS3, pEF-Core, FLAG-Δprotease, FLAG-ΔPH 2, and FLAG-ΔH 1 were expressed in 293T cells treated with 17-AAG. Proteins immunoprecipitated with anti-core, Hsp90 antibody were analyzed by Western blotting. 17-AAG-treated cell lysates were analyzed on Western blots, using the specific antibodies shown to the *right* of the panels. *Lane 1*, control; *lane 2*, 17-AAG (1 μM).

3*B*). However, when 50 nM 17-AAG was added to the cells at 3-day intervals for 15 days (*black squares*), the observed significant reduction in HCV RNA (by 3 log) was sustained from day 3 to day 15. We used trypan blue staining to check that long term treatment with 17-AAG did not induce cellular toxicity (Fig. 3*A*). Our results suggested that 17-AAG has the potential to safely induce long term suppression in HCV replication.

Reduced Expression of NS3 Protein in 17-AAG-treated HCV Replicon Cells—To investigate the mechanism by which 17-AAG inhibited HCV replication, we analyzed the expression of HCV core, E1, E2, NS3, NS4A, NS4B, NS5A, and NS5B proteins by Western blotting. NNC#2 cells treated with increasing doses of 17-AAG showed a marked reduction in the expression of NS3 (Fig. 4*A*) after 3 days, in common with the level of HCV RNA (Fig. 2*A*). However, levels of the other proteins were unchanged. This dose-dependent inhibition suggested that NS3 was more sensitive to 17-AAG than the other proteins. Similar effects on NS3 expression and RNA replication were seen in #50-1 cells treated with 17-AAG (Fig. 4*A*).

Another effect of 17-AAG treatment seen in these cells was an increase in Hsp70 expression and a slight increase in Hsp90 expression (Fig. 4*B*). The induction of Hsp70 expression suggested that Hsp90 inhibition by 17-AAG strongly activated HSF-1 (heat-shock transcription factor 1) (43). We also examined the levels of HCV core and NS5B protein expression in NNC#2 cells treated with 50 nM 17-AAG. Reduced levels of these proteins were seen in NNC#2 cells on day 6, and both HCV core and NS5B protein were undetectable on day 9 (Fig. 4*C*). To determine whether 17-AAG promoted the degradation of NS3, we next looked at the effect of 17-AAG on #50-1 cells in which proteasomal degradation was also inhibited. Although 17-AAG treatment still induced a reduction in the NS3 protein level in #50-1 cells (Fig. 4*D*), the degradation of NS3 was completely blocked in the presence of the proteasome inhibitor, MG132. This suggested that the pharmacological effect of 17-AAG was dependent on the proteasome system (44, 45).

Protein Folding in Hsp90-NS3 Interaction—To investigate the role of Hsp90 in HCV NS3 activation, the FLAG-NS3 protein was transfected into 293T cells, with or without 17-AAG, and the cell lysates were analyzed by Western blotting. The expression of NS3 from FLAG-NS3 was reduced in the presence of 17-AAG (Fig. 5*A*), suggesting that Hsp90 is involved in HCV NS3 degradation, possibly through a physical interaction.

We confirmed this specific interaction by immunoprecipitating 293T cell lysates with anti-FLAG antibody. This clearly showed that FLAG and Hsp90 co-precipitated, suggesting that NS3 was bound to the chaperone complex formed with Hsp90 (Fig. 5*B*). NS3 mutants lacking the protease and helicase regions were generated in order to identify the region responsible for the interaction with Hsp90 (Fig. 5*C*). FLAG-NS3, FLAG-NS3-Δhelicase, or FLAG-NS3-Δprotease were transfected into 293T cells, and anti-FLAG antibody immunoprecipitates were analyzed by Western blotting (Fig. 5*D*). Although FLAG-NS3-Δprotease was clearly co-immunoprecipitated with Hsp90, no protein band corresponding to FLAG-NS3-Δhelicase was detected (Fig. 5*D*), suggesting that the NS3 helicase region mediates binding to Hsp90. To confirm this finding, plasmids expressing different NS3 helicase mutants fused with FLAG (ΔPH 1, ΔPH 2, and ΔH 1) were constructed (Fig. 5*E*). Expressing these NS3 helicase mutants in 293T cells and analyzing their immunoprecipitates with anti-FLAG antibody by Western blotting showed that, although all of the NS3 helicase mutant proteins were immunoprecipitated by anti-FLAG-antibody, no Hsp90 was co-precipitated (Fig. 5*F*).

We also confirmed that the NS3 helicase region mediated the specific interaction with Hsp90 by transfecting FLAG-NS3 and FLAG-NS3 deletion mutants into 293T cells pretreated with 17-AAG (Fig. 5*G*). The proteins expressed by FLAG-NS3 and FLAG-NS3-Δprotease were degraded in cells pretreated with 17-AAG, whereas no degradation of the ΔPH 2 and ΔH 1 NS3 mutants lacking helicase regions was seen (Fig. 5*G*). Further, when pEF-core was expressed in 293T cells, core was unable to co-immunoprecipitate Hsp90, and no degradation of core protein was observed (Fig. 5*G*). Our data demonstrate that 17-AGG destabilizes several binding proteins (NS3 and NS3-Δprotease) to Hsp90 but stablilizes some nonbinding proteins (the ΔPH 2 and ΔH 1 NS3 mutants lacking helicase regions and core) to Hsp90. In previous reports (46), similar effects were observed when wild-type and mutated p53 were translated in the presence of geldanamycin. These results further supported the hypothesis that Hsp90 has a role in folding the NS3 helicase domain and that this has an important role in stabilizing the full-length NS3 protein. A protein complex that includes NS3 and Hsp90 is therefore implicated in the control of HCV replication.

DISCUSSION

The Hsp90 inhibitor, 17-AAG, is known to have highly selective effects on tumor cells that are a result of its high affinity for Hsp90 client oncoproteins, which are incorporated into the Hsp90-dependent multichaperone complex, thereby increasing their binding affinity for 17-AAG more than 100-fold (47). This high selectivity effectively minimizes the toxic side effects of 17-AAG so that it is a good candidate for clinical application, especially in treating neurodegenerative diseases. In this study, we observed the inhibitory effects of 17-AAG on the replication of an HCV subgenomic replicon that lacked NS2. On the other hand, Waxman *et al.* (37) demonstrated a role for Hsp90 in promoting the cleavage of HCV NS2/3 protein using NS2/3 translated in rabbit reticulocyte lysate and expressed in Jurkat cells. Because the replicon cells used in our study genetically lacked NS2, our results suggest that Hsp90 may directly interact with the NS3 protein in the HCV replicon.

In cell lines in which 17-AAG was a potent inhibitor of HCV replication, with IC_{50} values of 3–10 nM, we also found strong evidence that the association between HCV Hsp90 and NS3, but not other NS proteins, was the essential mechanism controlling the preferential degradation of NS3 after 17-AAG treatments. Furthermore, we showed that NS3 interacted with Hsp90 through the NS3 helicase domain. It was also clear that the expression of NS3 protein with helicase activity in 293T cells pretreated with 17-AAG was reduced, but the expression of NS3 mutants lacking the helicase regions (ΔPH 2 and ΔH 1) was not. The role of Hsp90 in achieving and/or stabilizing the NS3 protein was suggested by the fact that only 17-AGG bound to Hsp90 was capable of affecting NS3. The use of Hsp90 inhibitors represents a novel strategy for the development of anti-HCV therapies.

Acknowledgments—We are grateful to M. Sato, R. Tobita, and Y. Katumura for excellent technical assistance.

REFERENCES

1. Alter, H. J., Purcell, R. H., Shih, J. W., Melpolder, J. C., Houghton, M., Choo, Q. L., and Kuo, G. (1989) *N. Engl. J. Med.* **321,** 1494–1500
2. Choo, Q. L., Kuo, G., Weiner, A. J, Overby, L. R., Bradley, D. W., and Houghton, M. (1989) *Science* **244,** 359–362
3. McHutchison, J. G., Gordon, S. C., Schiff, E. R., Shiffman, M. L., Lee, W. M., Rustgi, V. K., Goodman, Z. D., Ling, M. H., Cort. S., and Albrecht, J. K. (1998) *N. Engl. J. Med.* **339,** 1485–1492
4. Glue, P., Rouzier-Panis, R., Raffanel, C., Sabo, R., Gupta, S. K., Salfi, M., Jacobs, S., and Clement, R. P. (2000) *Hepatology* **32,** 647–653
5. Saito, I., Miyamura, T., Ohbayashi, A., Harada, H., Katayama, T., Kikuchi, S., Watanabe, Y., Koi, S., Onji, M., and Ohtaet, Y. (1990) *Proc. Natl. Acad. Sci. U. S. A.* **87,** 6547–6549
6. Seeff, L. B. (1997) *Hepatology* **26,** 21S–28S
7. Bartenschlager, R., and Lohmann, V. (2001) *Antiviral Res.* **52,** 1–17
8. Taylor, D. R., Shi, S. T., Romano, P. R., Barber, G. N., and Lai, M. M. (1999) *Science* **285,** 107–110
9. Grakoui, A., Wychowski, C., Lin. C., Feinstone, S. M., and Rice, C. M. (1993) *J. Virol.* **67,** 1385–1395
10. Hijikata, M., Mizushima, H., Akagi, T., Mori, S., Kakiuchi, N., Kato, N., Tanaka, T., Kimura, K., and Shimotohno, K. (1993) *J. Virol.* **67,** 4665–4675
11. Grakoui, A., McCourt, D. W., Wychowski, C., Feinstone, S. M., and Rice, C. M. (1993) *Proc. Natl. Acad. Sci. U. S. A.* **90,** 10583–10587
12. Bartenschlager, R., Ahlborn-Laake, L., Mous, J., and Jacobsen, H. (1993) *J. Virol.* **67,** 3835–3844
13. Grakoui, A., McCourt, D. W., Wychowski, C., Feinstone, S. M., and Rice, C. M. (1993) *J. Virol.* **67,** 2832–2843
14. Bartenschlager, R., Lohmann, V., Wilkinson, T., and Koch, J. O. (1995) *J. Virol.* **69,** 7519–7528
15. Failla, C., Tomei, L., and De Francesco, F. (1995) *J. Virol.* **69,** 1769–1777
16. Lin, C., Thomson, J. A., and Rice, C. M. (1995) *J. Virol.* **69,** 4373–4380
17. Tanji, Y., Hijikata, M., Satoh, S., Kaneko, T., and Shimotohno, K. (1995) *J. Virol.* **69,** 1575–1581
18. Egger, D., Wolk, B., Gosert, R., Bianchi, L., Blum, H. E., Moradpour, D., and Bienz, K. (2002) *J. Virol.* **76,** 5974–5984
19. Gosert, R., Egger, D., Lohmann, V., Bartenschlager, R., Blum, H. E., Bienz, K., and Moradpour, D. (2003) *J. Virol.* **77,** 5487–5492
20. Blight, K. J., Kolykhalov, A. A., and Rice, C. M. (2000) *Science* **290,** 1972–1974
21. Guo, J. T., Bichko, V. V., and Seeger, C. (2001) *J. Virol.* **75,** 8516–8523
22. Krieger, N., Lohmann, V., and Bartenschlager, R. (2001) *J. Virol.* **75,** 4614–4624

23. Lohmann, V., Hoffmann, S., Herian, U., Penin, F., and Bartenschlager, R. (2003) *J. Virol.* **77,** 3007–3019
24. Behrens, S. E., Tomei, L., and De Francesco, R. (1996) *EMBO J.* **15,** 12–22
25. Lohmann, V., Korner, F., Herian, U., and Bartenschlager, R. (1997) *J. Virol.* **71,** 8416–8428
26. Friebe, P., and Bartenschlager, R. (2002) *J. Virol.* **76,** 5326–5338
27. Kolykhalov, A. A., Mihalik, K., Feinstone, S. M., and Rice, C. M. (2000) *J. Virol.* **74,** 2046–2051
28. Yanagi, M., St. Claire, M., Emerson, S. U., and Purcell Bukh, J. (1999) *Proc. Natl. Acad. Sci. U. S. A.* **96,** 2291–2295
29. Yi, M., and Lemon, S. M. (2003) *J. Virol.* **77,** 3557–3568
30. Picard, D. (2002) *Cell Mol. Life Sci.* **59,** 1640–1648
31. Wegele, H., Muller, L., and Buchner, J. (2004) *Rev. Physiol. Biochem. Pharmacol.* **151,** 1–44
32. Pratt, W. B., and Toft, D. O. (2003) *Exp. Biol. Med.* **228,** 111–133
33. Smith, D. F., Whitesell, L., and Katsanis, E. (1998) *Pharmacol. Rev.* **50,** 493–514
34. McClellan, A. J., and Frydaman, J (2001) *Nat. Cell Biol.* **3,** E1–E3
35. Grenert, J. P., Sullivan, W. P., Fadden, P., Haystead, T. A., Clark, J., Mimnaugh, E., Krutzsch, H., Ochel, H. J., Schulte, T. W., Sausville, E., Neckers, L. M., and Toft, D. O. (1997) *J. Biol. Chem.* **272,** 23843–23850
36. Supko, J. G., Hickman, R. L., Grever, M. R., and Malspeis, L. (1995) *Cancer Chemother. Pharmacol.* **36,** 305–315
37. Waxman, L., Whitney, M., Pollok, B. A., Kuo, L. C., and Darke, P. L. (2001) *Proc. Natl. Acad. Sci. U. S. A.* **98,** 13931–13935
38. Nakagawa, S., Umehara, T., Matsuda, C., Kuge, S., Sudoh, M., and Kohara, M. (2007) *Biochem. Biophys. Res. Commun.* **353,** 882–888
39. Okamoto, T., Nishimura, Y., Ichimura, T., Suzuki, K., Miyamura, T., Suzuki, T., Moriishi, K., and Matsuura, Y. (2006) *EMBO J.* **25,** 5015–5025
40. Kishine, H., Sugiyama, K., Hijikata, M., Kato, N., Takahashi, H., Noshi, T., Nio, Y., Hosaka, M., Miyanari, Y., and Shimotohno, K. (2002) *Biochem. Biophys. Res. Commun.* **290,** 993–999
41. Ishii, N., Watashi, K., Hishiki, T., Goto, K., Inoue, D., Hijikata, M., Wakita, T., Kato, N., and Shimotohno, K. (2006) *J. Virol.* **80,** 4510–4520
42. Takeuchi, T., Katsume, A., Tanaka, T., Abe, A., Inoue, K., Tsukiyama-kohara, K., Kawaguchi, R., Tanaka, S., and Kohara, M. (1999) *Gastroenterology* **11,** 636–642
43. Sittler, A., Lurz, R., Ueder, G., Priller, J., Lehrach, H., Hayer-Hartl, M. K., Hartl, F. U., and Wanker, E. E. (2001) *Hum. Mol. Genet.* **10,** 1307–1315
44. Bonvini, P., Dalla Rosa, H., Vignes, N., and Rosolen, A. (2004) *Cancer Res.* **64,** 3256–3264
45. Mimnaugh, E. G., Chavany, C., and Neckers, L. (1996) *J. Biol. Chem.* **271,** 22796–22801
46. Blagosklonny, M. V., Toretsky, J., Bohen, S., and Neckers L. (1996) *Proc. Natl. Acad. Sci. U. S. A.* **93,** 8379–8383
47. Kamal, A., Thao, L., Sensintaffar, J., Zhang, L., Boehm, M. F., Fritz, L. C., and Burrows, F. J. (2003) *Nature* **425,** 357–359

Sequence Variation in Hepatitis C Virus Nonstructural Protein 5A Predicts Clinical Outcome of Pegylated Interferon/Ribavirin Combination Therapy

Ahmed El-Shamy,[1] Motoko Nagano-Fujii,[1] Noriko Sasase,[2] Susumu Imoto,[2] Soo-Ryang Kim,[2] and Hak Hotta[1,3]

A substantial proportion of hepatitis C virus (HCV)-1b–infected patients still do not respond to interferon-based therapy. This study aims to explore a predictive marker for the ultimate virological response of HCV-1b–infected patients treated with pegylated interferon/ribavirin (PEG-IFN/RBV) combination therapy. Nonstructural protein 5A (NS5A) sequences of HCV in the pretreated sera of 45 patients infected with HCV-1b were analyzed. The mean number of mutations in the variable region 3 (V3) plus its upstream flanking region of NS5A (amino acid 2334-2379), referred to as IFN/RBV resistance-determining region (IRRDR), was significantly higher for HCV isolates obtained from patients who later achieved sustained virological response (SVR) by PEG-IFN/RBV than for those in patients undergoing non-SVR. The receiver operating characteristic curve analysis estimated six mutations in IRRDR as the optimal threshold for SVR prediction. Indeed, 16 (76%) of 21 SVR, but only 2 (8%) of 24 non-SVR, had HCV with six or more mutations in IRRDR (IRRDR ≥ 6) ($P < 0.0001$). All of 18 patients infected with HCV of IRRDR of 6 or greater examined showed a significant (≥1 log) reduction or disappearance of serum HCV core antigen titers within 24 hours after initial dose of PEG-IFN/RBV, whereas 10 (37%) of 27 patients with HCV of IRRDR of 5 or less did ($P < 0.0001$). The positive predictive value of IRRDR of 6 or greater for SVR was 89% (16/18; $P = 0.0007$), with its negative predictive value for non-SVR being 81% (22/27; $P = 0.0008$). *Conclusion:* A high degree (≥6) of sequence variation in IRRDR would be a useful marker for predicting SVR, whereas a less diverse (≤5) IRRDR sequence predicts non-SVR. (HEPATOLOGY 2008;48:38-47.)

Hepatitis C virus (HCV) infection is the major cause of chronic hepatitis, liver cirrhosis, and hepatocellular carcinoma in industrialized countries. However, HCV infection is curable, and its complications can be prevented by antiviral therapy.[1,2] Currently, the most effective treatment of chronic HCV infection is based on a combination of pegylated interferon (PEG-IFN) and ribavirin (RBV).[3] Even with this treatment regimen, however, sustained virological response (SVR) rates for those infected with the most resistant genotypes, HCV-1a and HCV-1b, still hover at approximately 50%.[3,4] Considering the high cost and the significant side effects associated with this combination therapy, it is worthy to identify patients most likely to benefit from therapy.[5] Predictors of IFN-based therapy can be classified into two categories, pretreatment and on-treatment factors. Pretreatment factors comprise host factors, such as age, sex, obesity, ethanol consumption, hepatic iron overload, fibrosis, immune responses, and coinfection with other viruses, and viral factors, which mainly include viral genotypes and viral load. On-treatment factors are mainly related to the viral kinetics within

Abbreviations: aa, amino acid; CI, confidence interval; CNR, complete nonresponse; ETR, end-of-treatment response; EVR, early virological response; HCV, hepatitis C virus; IFN, interferon; IRRDR, interferon/ribavirin resistance-determining region; ISDR, interferon sensitivity-determining region; NS5A, nonstructural protein 5A; nt, nucleotide; PEG, pegylated; PKR-BD, double-stranded RNA-activated protein kinase-binding domain; RBV, ribavirin; RT-PCR, reverse transcription polymerase chain reaction; SVR, sustained virological response; V3, variable 3.

From the [1]Division of Microbiology, Kobe University Graduate School of Medicine, Kobe, Japan; [2]Division of Gastroenterology, Kobe Asahi Hospital, Kobe, Japan; and [3]International Center for Medical Research and Treatment, Kobe University Graduate School of Medicine, Kobe, Japan.

Received August 10, 2007; accepted March 11, 2008.

Supported in part by grants-in-aid for scientific research from the Ministry of Education, Culture, Sports, Science, and Technology and the Ministry of Health, Labour, and Welfare of Japan. This study was also carried out as part of the Program of Founding Research Centers for Emerging and Reemerging Infectious Diseases (Ministry of Education, Culture, Sports, Science and Technology) and the 21st Century Center of Excellence program at Kobe University Graduate School of Medicine.

Address reprint requests to: Hak Hotta, M.D., Ph.D., Division of Microbiology, Kobe University Graduate School of Medicine, 7-5-1 Kusunoki-cho, Chuo-ku, Kobe 650-0017, Japan. E-mail: hotta@kobe-u.ac.jp; fax: (81)-78-382-5519.

Published online in Wiley InterScience (www.interscience.wiley.com).

DOI 10.1002/hep.22339

Potential conflict of interest: Nothing to report.

the first few weeks of treatment.[6] Because the HCV genotype is one of the major factors affecting IFN-based therapy response, IFN resistance is, at least partly, genetically encoded by HCV itself.[7] In this context, nonstructural protein 5A (NS5A), one of the HCV nonstructural proteins, has been widely discussed for its correlation with IFN responsiveness. Enomoto et al.[8,9] proposed that the sequence variations within a region in NS5A, called the IFN sensitivity-determining region (ISDR), is correlated with IFN responsiveness. It was further demonstrated that ISDR and its adjacent sequence was able to bind to double-stranded RNA-activated protein kinase (PKR), one of the important antiviral proteins of the host cell, to inhibit its enzymatic activity and, therefore, the combined region is called PKR-binding domain (PKR-BD).[10,11] A significant correlation between sequence variation in PKR-BD and IFN responsiveness was also reported.[12] In addition, there are some reports that showed a correlation between IFN responsiveness and the sequence diversity of the variable region 3 (V3) [amino acids (aa) 2356 to 2379] or its surrounding regions near the carboxy terminus of NS5A.[12-20]

We have recently reported that a high degree of sequence variations in the V3 and the pre-V3 regions (aa 2334-2355) of NS5A, which we collectively refer to as IFN/RBV resistance-determining region (IRRDR) (aa 2334-2379), was closely correlated with early virological response (EVR) by week 16 in HCV-1b–infected patients treated with PEG-IFN and RBV.[21] In the current study, we aimed to follow up our previous observations to investigate whether the degree of sequence variation in IRRDR could also correlate with SVR on PEG-IFN/RBV combination therapy.

Patients and Methods

Patients. A total of 45 patients chronically infected with HCV-1b, whose diagnoses had been made based on anti-HCV antibody detection, HCV subtype determination according to the method by Okamoto et al.,[22] and clinical follow-up, were treated with PEG-IFN α-2b (1.5 μg/kg body weight, once weekly, subcutaneously) and RBV (600-800 mg daily, per os), according to a standard treatment protocol for Japanese patients established by a hepatitis study group of the Ministry of Health, Labour, and Welfare, Japan, at Kobe Asahi Hospital, Hyogo Prefecture, Japan. All the patients were confirmed negative for hepatitis B surface antigen using chemiluminescent immunoassay (Abbott Japan Co., Ltd., Tokyo, Japan). Serum samples were collected from the patients at intervals of 4 weeks before, during, and after the treatment, and tested for HCV RNA by reverse transcription polymerase chain reaction (RT-PCR), as reported previously.[21] The quantification of serum HCV RNA titers was performed by RT-PCR with an internal RNA standard derived from the 5′ noncoding region of HCV (Amplicor HCV Monitor test, version 2.0, Roche Diagnostics, Tokyo, Japan). The thresholds of the low-range and high-range measurements of this assay were 50 and 600 IU/mL, respectively. HCV core antigen in the sera was also quantitatively measured by chemiluminescent immunoassay (Abbott Japan Co., Ltd., Tokyo, Japan). The threshold of this assay is 20 fmol/L.

The study protocol was approved beforehand by the Ethic Committee in Kobe Asahi Hospital, and written informed consent was obtained from each patient before the treatment.

NS5A Sequence Analysis. HCV RNA was extracted from 140 μL serum using a commercially available kit (QIAmp viral RNA kit; QIAGEN, Tokyo, Japan). For amplification of the NS5A region of the HCV genome, the extracted RNA was reverse transcribed and amplified for full-length NS5A using SuperScript One-step RT-PCR for long templates (Invitrogen, Tokyo, Japan) and a set of primers, NS5A-F1 [5′-TACTCCCTGCCATCCTCTCTCCTG-3′; sense, nucleotides (nt) 5974-5997] and NS5A-F2 (5′-CTCCTTGAGCACGTCCCGGT-3′; antisense, nt 7777-7796). The resultant RT-PCR product was subjected to a second-round PCR by using Platinum Taq DNA polymerase (Invitrogen) and an inner set of primers, NS5A-F3 (5′TCTCCAGCCTTACCATCACYCA-3′; sense, nt 6172-6193) and NS5A-F4 (5′-CGGTARTGRTCGTCCAGGAC-3′; antisense, nt 7761-7780). The samples that were not amplifiable (nos. 3, 23, 47, 61, 65, and 69) using the aforementioned primers were amplified using primer sets reported previously.[23] Reverse transcription was performed at 45°C for 30 minutes and terminated at 94°C for 2 minutes, followed by the first-round PCR over 35 cycles, with each cycle consisting of denaturation at 94°C for 30 seconds, annealing at 55°C for 30 seconds and extension at 68°C for 90 seconds. The second-round PCR was performed under the same condition. The amplified fragments were purified with QIA quick PCR purification kit (QIAGEN), and visualized by agarose gel electrophoresis and ethidium bromide staining. The sequences of the amplified fragments were determined by direct sequencing without subcloning using Big Dye Deoxy Terminator cycle sequencing kit and ABI 337 DNA sequencer (Applied Biosystems, Inc, Japan). The aa sequences were deduced and aligned using GENETYX Win software version.7.0 (GENETYX Corp., Tokyo, Japan). Numbering of aa throughout the complete manuscript is according to the poly protein of HCV genotype 1b prototype HCV-J.[24]

Statistical Analysis. Statistical difference in the parameters, including all available patients' demographic, biochemical, hematological, and virological data as well as IRRDR sequence variations factors, was determined between different patients' groups by Student *t* test for numerical variables, and Fisher's exact probability test for categorical variables. In the case of multiple comparisons for various regions of NS5A, *P* values were adjusted by the Bonferroni method to reduce the probability of erroneously classifying nonsignificant hypothesis as significant. Although there are five regions of comparison (full-NS5A, N-half, ISDR, PKR-BD and IRRDR), the ISDR is entirely within the PKR-BD, and all the regions fall within the full-NS5A. Therefore, it would be reasonable to adjust the *P* values for three regions of comparison. Accordingly, the *P* value for a test was multiplied by 3. To evaluate the optimal threshold of IRRDR mutations for SVR prediction, the receiver operating characteristic curve was constructed and the area under the curve as well as the sensitivity and specificity were calculated. Subsequently, univariate and multivariate logistic analyses were performed to identify variables that independently predict SVR. The odds ratios and 95% confidence intervals (95% CI) were also calculated. Kaplan-Meier HCV survival curve analysis was performed based on serum HCV-RNA positivity data during treatment period (48 weeks) according to the number of IRRDR mutations (IRRDR $\geq$ 6 and IRRDR $\leq$ 5). The HCV death event was estimated as the first time point of HCV-RNA clearance after initiation of the treatment. The data obtained were evaluated by the log-rank test. Positive and negative predictive values of SVR predictors were computed, and their significance levels were evaluated using the sign test. All statistical analyses were performed using the SPSS version 16 software (SPSS Inc., Chicago, IL). Unless otherwise stated, a *P* value of less than 0.05 was considered statistically significant.

Nucleotide Sequence Accession Numbers. The sequence data reported in this article have been deposited in the DDBJ/EMBL/GenBank nucleotide sequence databases with the accession numbers AB285035 through AB285081, and AB354116 through AB354118.

Results

Virological Responses of the Patients Treated with PEG-IFN and RBV. Proportions of various virological responses of the patients treated with PEG-IFN/RBV combination therapy are shown in Table 1. Of 45 patients enrolled in this study, 23 (51%), 31 (69%), and 21 (47%) patients, respectively, achieved EVR by week 12 [EVR(12w)], end-of-treatment response (ETR), and sustained virological response (SVR). Among 23 patients with EVR(12w), 22 (96%) and 18 patients (78%) achieved ETR and SVR, respectively. This indicates that EVR(12w) was significantly correlated with ETR and SVR ($P < 0.0001$). A total of 24 patients (53%) failed to achieve SVR, and they were referred to as non-SVR. Non-SVR can be divided into two categories: (i) complete nonresponse (CNR), which is defined by continued presence of serum HCV RNA up to the end of the treatment, and (ii) relapse, which is defined by transient disappearance of HCV RNA at a certain time point followed by reappearance of HCV RNA either before or after the end of the treatment. CNR represented 24% (11/45) of all cases and 46% (11/24) of non-SVR. Thirteen (29%) of 45 patients underwent relapse. Among 13 relapsers, 3 (23%) patients had rebound in HCV viremia before the end of the treatment and, hence, were defined as undergoing viral breakthrough, whereas 10 (77%) patients had rebound in HCV viremia after the end of the treatment, defined as ETR-relapsers.

Table 1. Proportions of Various Virological Responses of Patients Treated With PEG-IFN/RBV

Virological Response	Proportion
EVR(12w)	51% (23/45)*
ETR	69% (31/45)
SVR	47% (21/45)
Non-SVR	53% (24/45)
CNR	24% (11/45)
Relapse	29% (13/45)
ETR-relapse	22% (10/45)
Viral breakthrough	7% (3/45)

*No. of patients/no. of total.

Abbreviations: PEG-IFN/RBV, pegylated-interferon/ribavirin; EVR, early virological response; ETR, end-of-treatment response; SVR, sustained virological response; CNR, complete nonresponse.

Demographic characteristics of patients with SVR, non-SVR, CNR, and relapse are summarized in Table 2. Age, sex, body weight, hemoglobin levels, or gamma guanosine triphosphate titers did not significantly differ between SVR and non-SVR or CNR. However, patients with SVR showed a trend toward having significantly higher platelet counts than those with non-SVR and CNR. Also, the mean initial titers of HCV core antigen for non-SVR and CNR, respectively, were 1.6 times and 2.3 times higher than that for SVR, although the difference was not statistically significant. HCV RNA titers were almost the same among them.

Correlation Between Virological Responses and the Sequence Variation of IRRDR of HCV NS5A Obtained from the Pretreated Sera. The entire NS5A region of the HCV genome was amplified from the pretreated sera and the aa sequences deduced. We compared

Table 2. Demographic Characteristics of Patients With SVR, Non-SVR, CNR, and Relapse

Factor	SVR	Non-SVR	CNR	Relapse	P Value		
					SVR versus Non-SVR	SVR versus CNR	SVR versus Relapse
Age	56.5 ± 8.0*	59.9 ± 10.6	59.4 ± 10.0	60.3 ± 11.5	NS†	NS	NS
Sex (male/female)	12/9	13/11	6/5	7/6	NS	NS	NS
Body weight (kg)	58.5 ± 9.4	59 ± 13.2	61.0 ± 10.8	57.8 ± 15.3	NS	NS	NS
Platelets ($\times 10^4/mm^3$)	18.3 ± 4.4	15.0 ± 4.9	12.3 ± 3.9	16.8 ± 4.9	0.02‡	0.001‡	NS
Hemoglobin (g/dL)	14.1 ± 1.3	13.7 ± 1.4	14.4 ± 1.3	14.3 ± 1.5	NS	NS	NS
γ-GTP (IU/L)	43.5 ± 28.7	51.6 ± 35.7	62.8 ± 40.3	43.8 ± 30.5	NS	NS	NS
HCV-RNA (KIU/mL)	1326 ± 1256	1667 ± 1311	1488 ± 1228	1818 ± 1408	NS	NS	NS
HCV core antigen (fmol/L)	6183 ± 6894	9830 ± 1214	14,033 ± 17,089	6481 ± 4023	NS	NS	NS

*Mean ± SD.
†Not significant.
‡Student *t* test.
Abbreviations: SVR, sustained virological response; CNR, complete nonresponse; γ-GTP, gamma guanosine triphosphate.

each NS5A sequence with a consensus sequence inferred from aligning the previously published NS5A-1b sequences.[8] In this connection, the consensus sequence for IRRDR differs from the corresponding sequence of a prototype strain of IFN resistance HCV-1b (HCV-J; DDBJ/EMBL/Genbank accession no. D90208) by a single residue at position 2367 (Ala instead of Gly). Because Ala^{2367} was conserved in 95% of the reported sequences, we used the IRRDR consensus sequence in this study. As shown in Table 3, the mean number of aa substitutions in the entire NS5A obtained from patients with SVR was significantly greater compared with non-SVR and relapse. There was no difference in the number of mutations in an N-terminal half of NS5A (aa 1972-2208), the ISDR (aa 2209-2248) or the PKR-BD (aa 2209-2274) between the different patients' groups. Conversely, we found a more obvious significant difference in the mean numbers of aa mutations within a region consisting of the pre-V3 and V3 regions, which we refer to as IRRDR, between SVR and other patients' groups (Table 3).

To estimate a cutoff number of mutations in IRRDR predicting SVR, the receiver operating characteristics analysis was performed. The result revealed that six mutations were an optimal number of mutations to predict SVR, because it achieved the highest sensitivity (76%) combined with the highest specificity (92%) and yielded an area under the curve of 0.81 (Fig. 1).

Indeed, only 2 (8%) of 24 patients with non-SVR, in contrast to 16 (76%) of 21 patients with SVR, had HCV with IRRDR of 6 or greater, with the difference between the two groups being statistically significant ($P < 0.0001$) (Table 4). Furthermore, none of 11 patients with CNR had HCV of IRRDR of 6 or greater, and the difference between SVR and CNR was statistically significant ($P < 0.0001$). Similarly, only 2 (15%) of 13 relapsers (10 ETR-relapsers + 3 patients with viral breakthrough) had HCV of IRRDR greater than or equal to 6, with the result demonstrating significant difference between SVR and relapse ($P = 0.001$).

Table 3. Average Numbers of aa Mutations Within Different Regions of HCV NS5A Obtained From Pretreated Sera of Patients With SVR, Non-SVR, CNR, and Relapse

NS5A Region	No. of Mutations*				P Value†		
	SVR	Non-SVR	CNR	Relapse	SVR versus Non-SVR	SVR versus CNR	SVR versus Relapse
Full-NS5A (aa 1972-2419)	24.9 ± 6.1*	19.7 ± 4.3	20.1 ± 5.2	19.4 ± 3.5	0.012	0.144	0.03
N-half (aa 1972-2208)	9.2 ± 1.9	8.6 ± 1.9	9.0 ± 2.4	8.2 ± 1.2	NS‡	NS	NS
ISDR (aa 2209-2248)	2.1 ± 2.8	1.2 ± 1.1	1.7 ± 1.4	0.8 ± 0.7	NS	NS	NS
PKR-BD (aa 2209-2274)	3.8 ± 3.4	2.5 ± 2.0	2.9 ± 2.4	2.1 ± 1.5	NS	NS	NS
IRRDR (aa 2334-2379)	6.1 ± 2.1	3.9 ± 1.4	3.7 ± 0.9	4.0 ± 1.8	0.0006	0.003	0.018

*Mean ± SD.
†The *P* values obtained with Student *t* test were adjusted using the Bonferroni method (see Materials and Methods).
‡Not significant.
Abbreviations: SVR, sustained virological response; CNR, complete nonresponse; aa, amino acid; ISDR: interferon sensitivity-determining region; PKR-BD, double-stranded RNA-activated protein kinase-binding domain; IRRDR, interferon/ribavirin resistance-determining region.

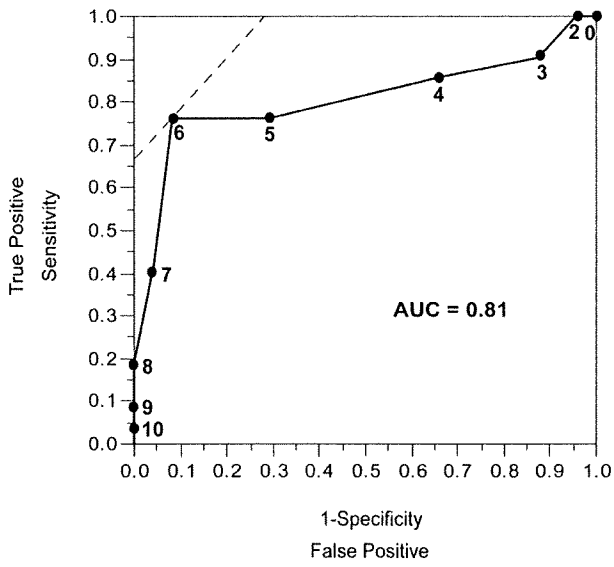

Fig. 1. The receiver operating characteristic curve analysis of IRRDR sequence variation for SVR prediction. The curve depicted with solid line shows an area under the curve of 0.81. Solid circles with numerals plotted on the curve represent different numbers of IRRDR mutations analyzed. The dashed line in the upper left corner indicates the optimal number of IRRDR mutations for SVR prediction, which yields the highest sensitivity (76%) and the highest specificity (92%).

When the IRRDR sequences obtained from all 45 patients were aligned along with the consensus sequence (Fig. 2), we noticed that 10 (48%) of 21 patients with SVR had alanine at position 2360 (Ala^{2360}), whereas only 3 (13%) of 24 patients with non-SVR and none of 11 patients with CNR did ($P = 0.02$ and 0.006, respectively) (Table 4). Similarly, 9 (43%) of 21 patients with SVR had threonine at position 2378 (Thr^{2378}), whereas only 3 (13%) of 24 patients with non-SVR and none of 11 patients with CNR did ($P = 0.04$ and 0.01, respectively).

To identify significant independent SVR predictors, we first entered all available baseline patients' features and IRRDR sequence variations data in univariate logistic analysis. As had been expected, this analysis yielded four factors significantly associated with SVR: IRRDR mutations, either continuous variable ($P < 0.0001$) or dichotomized at 6 ($P < 0.0001$), Ala^{2360} ($P = 0.002$), Thr^{2378} ($P = 0.019$), and platelet count ($P = 0.017$). Subsequently, we analyzed these four factors by multivariate logistic analysis. When the IRRDR mutations were dichotomized at 6, the multivariate analysis identified only the IRRDR of 6 or greater criterion as the independent predictor of SVR (odds ratio = 16.0; CI, 2.4-104.3; $P = 0.004$) (Table 5). However, when the IRRDR mutations were analyzed as a continuous variable, the multivariate analysis yielded IRRDR mutations (odds ratio = 1.8; CI, 1.1-3.1; $P = 0.02$) and Ala^{2360} (odds ratio = 9.3; CI, 1.1-78.8; $P = 0.04$) as independent SVR predictors.

Figure 3A shows the viral clearance rates of patients infected with HCV of IRRDR of 6 or greater and those with IRRDR of 5 or less at 4-week intervals during the whole observation period (72 weeks). All of 18 patients infected with HCV of IRRDR 6 or greater cleared the virus by week 16 and remained free of viremia thereafter until the end of the PEG-IFN/RBV treatment (week 48). Within 4 weeks after the cessation of the combination therapy, however, 2 (11%) of the 18 patients underwent relapse (ETR relapse). Conversely, 16 (59%) of the 27 patients with HCV of IRRDR of 5 or less cleared the virus by week 32. Of the 16 patients who once cleared the virus, 3 (19%) and 8 (50%) underwent relapse to become viral breakthrough and ETR relapsers, respectively.

Kaplan-Meier HCV survival curve analysis confirmed that, after the initiation of the IFN/RBV treatment, HCV clearance was achieved significantly more rapidly in patients infected with HCV isolates with IRRDR of 6 or greater than those with IRRDR of 5 or less, with the difference between the two groups being statistically significant ($P < 0.0001$) (Fig. 3B).

Sequence Analysis of ISDR and PKR-BD of HCV NS5A Obtained from Pretreated Sera. As described, there was no difference in the mean number of mutations in ISDR or PKR-BD between SVR and non-SVR or CNR (Table 3). Only four patients had HCV with four or

Table 4. Correlation Between NS5A Sequence Variation and Virological Responses of the Patients

	No. of Subjects / no. of Total*				P Value†		
Criteria	SVR	Non-SVR	CNR	Relapse	SVR versus Non-SVR	SVR versus CNR	SVR versus Relapse
IRRDR ≥ 6	16/21 (76%)	2/24 (8%)	0/11 (0%)	2/13 (15%)	< 0.0001	< 0.0001	0.001
Ala^{2360}	10/21 (48%)	3/24 (13%)	0/11 (0%)	3/13 (23%)	0.02	0.006	NS‡
Thr^{2378}	9/21 (43%)	3/24 (13%)	0/11 (0%)	3/13 (23%)	0.04	0.01	NS

*Total no. of SVR, Non-SVR, CNR, or relapse.

†Fisher's exact test.

‡Not significant.

Abbreviations: SVR, sustained virological response; CNR, complete nonresponse; IRRDR, interferon/ribavirin resistance-determining region; Ala^{2360}, alanine at position 2360; Thr^{2378}, threonine at position 2378.

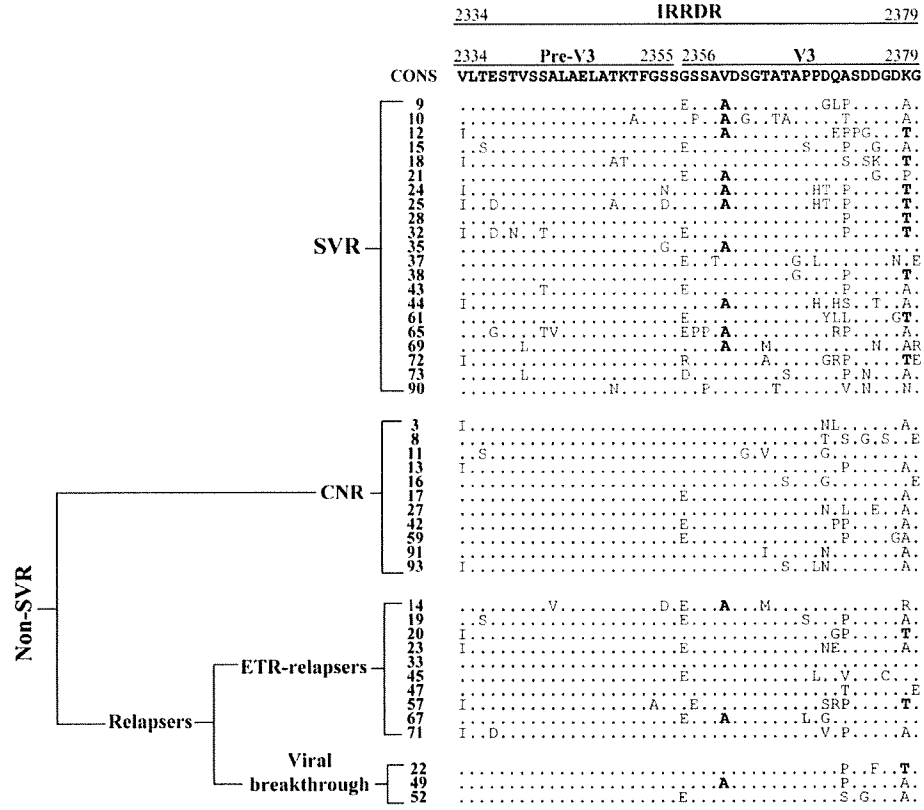

Fig. 2. Sequence alignment of IRRDR (Pre-V3 plus V3 regions) of NS5A of HCV-1b obtained from the pretreatment sera. The consensus sequence (Cons) is shown on the top. The Cons sequence differs from a prototype sequence of IFN-resistant HCV-1b (HCV-J; DDBJ/EMBL/GenBank accession no. D90208) by a single residue at position 2367 (alanine instead of glycine). The numbers along the sequence indicate aa positions. Dots indicate residues identical to those of the Cons sequence. Ala^{2360} and Thr^{2378} are written in boldface.

more mutations in ISDR (data not shown), the criterion for IFN-sensitive HCV strains according to Enomoto et al.[8,9] Although there appeared to be a trend for patients with HCV having four or more mutations in ISDR toward SVR (3 of 4), the difference was not statistically significant. Also, the prevalence of HCV with four or more mutations in ISDR was not significantly different between SVR (3 of 21; 14.3%) and non-SVR (1 of 24; 4.2%). It would be interesting to note, however, that all three HCV strains with four or more mutations in ISDR obtained from SVR (nos. 10, 65, and 72) had HCV of IRRDR of 6 or greater, whereas the only one strain with four or more mutations in ISDR from non-SVR (no. 13) had three mutations in IRRDR (data not shown). It is thus possible that the IRRDR sequence variation is associated with PEG-IFN/RBV responsiveness more closely than is the ISDR variation.

Table 5. Multivariate Logistic Regression Analysis to Identify Independent SVR Predictors

Factor	Odds (95% CI)	*P* value
Multivariate analysis 1		
IRRDR ≥ 6	16.0 (2.4-104.3)	0.004
Ala^{2360}	7.1 (0.8-66.8)	0.09
Thr^{2378}	4.1 (0.5-30.9)	0.17
Platelets	1.1 (0.9-1.4)	0.27
Multivariate analysis 2		
IRRDR mutations as a continuous variable	1.8 (1.1-3.1)	0.02
Ala^{2360}	9.3 (1.1-78.8)	0.04
Thr^{2378}	4.9 (0.7-33.3)	0.1
Platelets	1.2 (1.0-1.5)	0.08

Only factors that were significantly associated with SVR in univariate analysis were included in multivariate logistic regression analysis.

Abbreviations: IRRDR, interferon/ribavirin resistance-determining region; Ala^{2360}, alanine at position 2360; Thr^{2378}, threonine at position 2378, CI; confidence interval.

Correlation Between Rapid Reduction of HCV Core Antigen Titers and the Sequence Variation in IRRDR of HCV NS5A Obtained from the Pretreated Sera. As stated before, there was no significant difference in the mean values of initial HCV core antigen titers between patients with SVR and those with non-SVR (Table 2). However, we observed a strong association of SVR with rapid reduction of HCV core antigen titers during the very early stages of treatment, that is, 24 hours and 1, 2, and 4 weeks after the initiation of treatment (data not shown). Therefore, we analyzed whether the degree of sequence variation in IRRDR correlated with the very rapid reduction (24 hours after the first dose of PEG-IFN/RBV) of HCV core antigen titers. The result obtained clearly demonstrated a significant correlation between IRRDR of 6 or greater and the very rapid reduction of HCV core antigen titers 24 hours and 1, 2, and 4 weeks

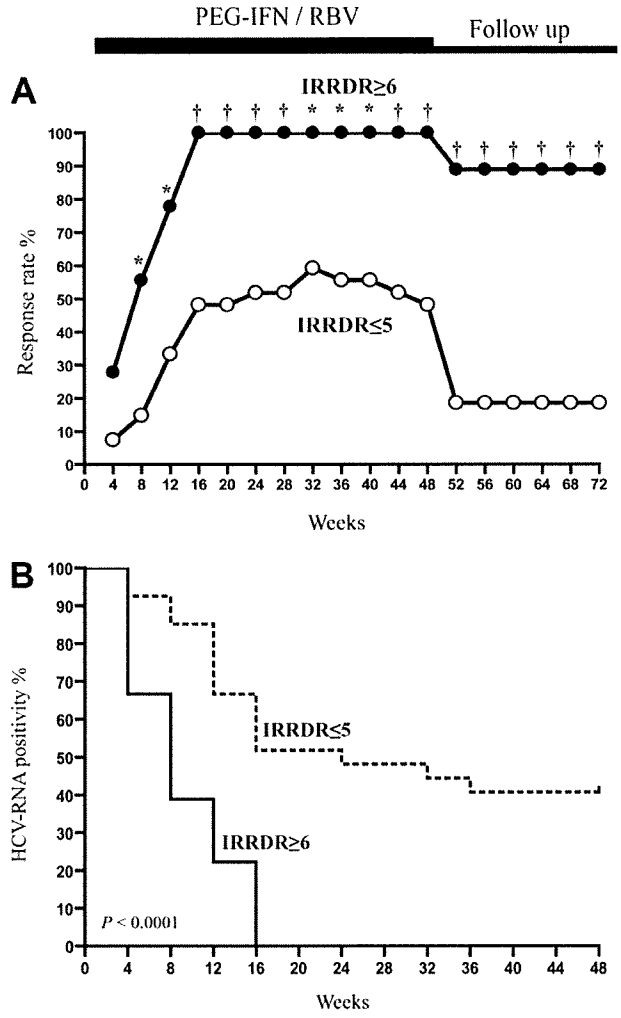

Fig. 3. Time course of HCV clearance during IFN/RBV treatment and follow-up period. (A) The viral clearance rates of patients infected with HCV isolates with six or more mutations in IRRDR (IRRDR ≥ 6) or five or fewer mutations (IRRDR ≤ 5) at 4-week intervals during the whole observation period. *$P < 0.01$; †, $P < 0.001$ (Fisher's exact probability test). (B) Kaplan-Meier HCV survival curve analysis based on serum HCV-RNA positivity during IFN/RBV treatment course (48 weeks) for HCV isolates with IRRDR of 6 or greater and IRRDR of 5 or fewer. $P < 0.0001$ (log-rank test).

after the initiation of treatment (Table 6). Most notably, all 18 patients infected with HCV isolates of IRRDR of 6 or greater achieved significant (≥1 log) reduction or disappearance of serum HCV core antigen titers 24 hours after the first dose of PEG-IFN/RBV.

Proposed Markers for Prediction of Various Virological Responses During PEG-IFN/RBV Combination Therapy. As described, IRRDR of 6 or greater and Ala^{2360} were statistically selected as independent SVR predictors. Therefore, we aimed to assess their predictability, in terms of positive and negative predictive values, for various virological responses to PEG-IFN/RBV combination therapy (Table 7). IRRDR greater than or equal to 6 could predict EVR(12w), ETR, and SVR with the positive predictive values of 78% ($P = 0.01$), 100% ($P = 0.000007$), and 89% ($P = 0.0007$), respectively. Moreover, the negative predictive value of IRRDR of 6 or greater for non-SVR was 81% ($P = 0.0008$). Thus, IRRDR of 6 or greater would be useful to predict not only SVR but also non-SVR. Similarly, Ala^{2360} could also predict ETR and SVR with positive predictive values of 92% ($P = 0.002$) and 77% ($P = 0.046$), respectively.

Discussion

A substantial proportion of HCV-1b–infected patients do not respond to IFN/RBV combination therapy. Given the significant side effects and high cost associated with this combination therapy, it would be of great utility if clinicians could predict, either before or during the treatment, which patients would, or would not, achieve SVR. Useful predictors of SVR must have a high positive predictive value; conversely, useful predictors of non-SVR must have high negative predictive value.[5] Most recent studies have focused on the possible correlation between the likelihood of achieving SVR and viral clearance kinetics during the first few months of the treatment.[25,26] Conversely, some studies dealt with the possible correlation between SVR and sequence variation within a part of NS5A, especially the V3 region.[12-20]

Table 6. Significant Correlation Between the Rapid Reduction of HCV Core Antigen Titers and IRRDR Sequence Variations

	No. of Patients With Significant Reduction of HCV Core Antigen Titers / No. of Total							
Criteria	24 Hours* (≥ 1 log)†	*P* Value‡	1 Week* (≥ 1 log)†	*P* Value‡	2 Weeks* (≥ 1.5 log)†	*P* Value‡	4 Weeks* (≥ 2 log)†	*P* Value‡
IRRDR ≥ 6	18/18	<0.0001	15/18	0.002	13/18	0.016	16/18	0.0007
IRRDR ≤ 5	10/27		9/27		9/27		10/27	

*Period after initiation of IFN/RBV therapy.

†Criteria of the significant reduction of HCV core antigen titers. Two (both at 24 hours and 1 week) and three patients (both at 2 and 4 weeks) who achieved disappearance of serum HCV core antigen were also considered to meet these criteria.

‡Fisher's exact test.

Abbreviations: IRRDR, interferon/ribavirin resistance-determining region; IFN/RBV, interferon/ribavirin.

Table 7. Positive Predictive Value, Negative Predictive Value, Sensitivity and Specificity of IRRDR ≥ 6 and Ala^{2360} on the Likelihood of Achieving Various Virological Responses

Virological Response	IRRDR ≥ 6				Ala^{2360}			
	PPV	NPV	Sensitivity	Specificity	PPV	NPV	Sensitivity	Specificity
EVR (12W)	78% (14/18)	67% (18/27)	61% (14/23)	82% (18/22)	69% (9/13)	56% (18/32)	39% (9/23)	82% (18/22)
ETR	100% (18/18)	56% (15/27)	58% (18/31)	100% (14/14)	92% (12/13)	41% (13/32)	39% (12/31)	93% (13/14)
SVR	89% (16/18)	81% (22/27)	76% (16/21)	92% (22/24)	77% (10/13)	66% (21/32)	48% (10/21)	88% (21/24)

Abbreviations: IRRDR, interferon/ribavirin resistance-determining region; Ala^{2360}, alanine at position 2360; EVR, early virological response; ETR, end-of-treatment response; SVR, sustained virological response; PPV, positive predictive value; NPV, negative predictive value.

We previously reported that a high degree of sequence variation (≥6 mutations) in IRRDR was significantly correlated with the EVR by week 16 in HCV-1b–infected patients treated with PEG-IFN/RBV combination therapy.[21] In the current follow-up study, we aimed to investigate whether the IRRDR sequence variation is correlated also with SVR. By using different statistical approaches, the results obtained clearly demonstrated that the high degree of sequence variation in IRRDR (IRRDR ≥6) significantly correlated with SVR, whereas the low degree of sequence variation in this region (IRRDR ≤5) correlated with non-SVR. Nearly two-thirds of patients with SVR had HCV of IRRDR of 6 or greater, whereas only 2 (8%) of 24 patients with non-SVR did ($P < 0.0001$) (Table 4). Notably, 16 of the 18 patients infected with HCV of IRRDR of 6 or greater achieved SVR. Accordingly, the positive predictive value and negative predictive value of IRRDR greater than or equal to 6 for SVR and non-SVR were 89% ($P = 0.0007$) and 81% ($P = 0.0008$), respectively (Table 7). Our current results thus strongly suggest that IRRDR greater than or equal to 6 would be a useful marker for prediction of SVR.

It was reported that the determination of HCV core antigen levels in the serum was an accurate and reliable alternative to monitor HCV RNA titers and that rapid reduction of HCV core antigen levels within a few weeks after the initiation of the therapy could predict treatment outcome in patients receiving PEG-IFN/RBV combination therapy.[27-29] Indeed, we found a strong association between the likelihood of achieving SVR and rapid reduction of HCV core antigen during the first 4 weeks of PEG-IFN/RBV combination therapy. More importantly, we found a significant correlation between the rapid reduction of HCV core antigen titers and the degree of sequence variation in IRRDR. Notably, all the patients infected with HCV of IRRDR greater than or equal to 6 showed a significant (≥1 log) reduction or disappearance of serum HCV core antigen titers 24 hours after the first dose of PEG-IFN/RBV (Table 6). This, in particular, suggests a possible influence of IRRDR of 6 or greater on HCV replication kinetics during IFN-based therapy because the direct effect of IFN begins a few hours after the first dose. Moreover, IRRDR greater than or equal to 6 was significantly associated with rapid clearance of serum HCV RNA as early as week 8 during PEG-IFN/RBV combination therapy (Fig. 3). These results collectively reinforce the possible correlation between the sequence variation in IRRDR and HCV clearance by the IFN-based therapy.

We also examined whether the criterion of IRRDR of 6 or greater was applicable to previously reported studies, for which information on both treatment outcome (responder versus nonresponder) and IRRDR sequences are available.[8,13] As shown in Table 8, the average numbers of amino acid variations from the same consensus sequence used in the current study were significantly larger for SVR than for non-SVR in a study with Japanese patients ($P = 0.003$)[8] and hovered at nearly a significant level in a study with European patients ($P = 0.06$).[13] More importantly, the criterion of IRRDR greater than or equal to 6 could significantly differentiate between responders and nonresponders in the Japanese study ($P = 0.003$) and also hovered at nearly a significant level in the European study ($P = 0.058$). It should be noted that, in the latter study, there were only three patients who had HCV with IRRDR of 6 or greater, all of whom became SVR. Taken together, these results suggest the useful application of IRRDR of 6 or greater as an SVR marker even in different geographical regions, although the prevalence of HCV with IRRDR of 6 or greater may vary with different regions of the world.

Although we observed significant correlation between the overall number of mutations in IRRDR and PEG-IFN/RBV responsiveness, we also found particular amino acid mutations, Ala^{2360} and Thr^{2378}, that were significantly associated with SVR (Table 4 and Fig. 2). In particular, Ala^{2360} was identified as an independent SVR marker. In this connection, it should be noted that four of five HCV isolates of IRRDR of 5 or less obtained from patients with SVR had either Ala^{2360} or Thr^{2378}. Furthermore, 20 (95%) of 21 HCV isolates obtained from pa-

Table 8. Comparative Analysis of the Mean Numbers of aa Mutations in IRRDR in Previously Reported Japanese and European Studies

Study	Factor	SVR	Non-SVR	*P* Value
Enomoto et al.[8]	No. of IRRDR mutations	7.6 ± 2.6*	3.7 ± 2.0	0.003†
	No. of patients with IRRDR ≥ 6	8	1	0.003‡
	IRRDR ≤ 5	1	8	
Duverlie et al.[13]	No. of IRRDR mutations	5.6 ± 2.3	4.2 ± 0.8	0.06†
	No. of patients with IRRDR ≥ 6	3	0	0.056‡
	IRRDR ≤ 5	5	11	
This study	No. of IRRDR mutations	6.1 ± 2.1	3.9 ± 1.4	0.0006†
	No. of patients with IRRDR ≥ 6	16	2	< 0.0001‡
	IRRDR ≤ 5	5	22	

NOTE. Same consensus sequence was used in this comparative analysis.
*Mean ± SD.
†Student *t* test.
‡Fisher's exact test.
Abbreviations: aa, amino acid; IRRDR, interferon/ribavirin resistance-determining region; SVR, sustained virological response.

tients with SVR had either one of the three factors (IRRDR ≥6, Ala^{2360}, or Thr^{2378}). To our knowledge, there is no known CD4 or CD8 epitope(s) in IRRDR so far reported. Interestingly, however, Neumann-Haefelin et al.[30] recently identified an HLA-A26 $CD8^+$ T-cell epitope located at position 2416, 37 aa distant from IRRDR. This epitope was shown to be targeted in all patients with acute resolving HCV infection examined. Further studies are needed to elucidate the role(s) for the distal carboxy terminal region of NS5A, including IRRDR, in both IFN/RBV responsiveness and T cell–mediated virus clearance.

In conclusion, our results suggest that a high degree of sequence variation in IRRDR (IRRDR ≥6), and a particular aa mutation (Ala^{2360}) to a lesser extent, would be a useful marker to predict SVR.

References

1. Hoofnagle JH, Seeff LB. Peginterferon and ribavirin for chronic hepatitis C. N Engl J Med 2006;355:2444-2451.
2. Pawlotsky JM. Therapy of hepatitis C: from empiricism to eradication. HEPATOLOGY 2006;43:S207-S220.
3. Manns MP, McHutchison JG, Gordon SC, Rustgi VK, Shiffman M, Reindollar R, et al. Peginterferon alfa-2b plus ribavirin compared with interferon alfa-2b plus ribavirin for initial treatment of chronic hepatitis C: a randomised trial. Lancet 2001;358:958-965.
4. Fried MW, Shiffman ML, Reddy KR, Smith C, Marinos G, Goncales FL Jr, et al. Peginterferon alfa-2a plus ribavirin for chronic hepatitis C virus infection. N Engl J Med 2002;347:975-982.
5. Ferenci P, Fried MW, Shiffman ML, Smith CI, Marinos G, Goncales FL Jr, et al. Predicting sustained virological responses in chronic hepatitis C patients treated with peginterferon alfa-2a (40 KD)/ribavirin. J Hepatol 2005;43:425-433.
6. Ferenci P. Predictors of response to therapy for chronic hepatitis C. Semin Liver Dis 2004;24(Suppl 2):25-31.
7. Welker MW, Hofmann WP, Welsch C, von Wagner M, Herrmann E, Lengauer T, et al. Correlation of amino acid variations within nonstructural 4B protein with initial viral kinetics during interferon-alpha-based therapy in HCV-1b-infected patients. J Viral Hepatol 2007;14:338-349.
8. Enomoto N, Sakuma I, Asahina Y, Kurosaki M, Murakami T, Yamamoto C, et al. Comparison of full-length sequences of interferon-sensitive and resistant hepatitis C virus 1b: sensitivity to interferon is conferred by amino acid substitutions in the NS5A region. J Clin Invest 1995;96:224-230.
9. Enomoto N, Sakuma I, Asahina Y, Kurosaki M, Murakami T, Yamamoto C, et al. Mutations in the nonstructural protein 5A gene and response to interferon in patients with chronic hepatitis C virus 1b infection. N Engl J Med 1996;334:77-81.
10. Gale MJ Jr, Korth MJ, Tang NM, Tan SL, Hopkins DA, Dever TE, et al. Evidence that hepatitis C virus resistance to interferon is mediated through repression of the PKR protein kinase by the nonstructural 5A protein. Virology 1997;230:217-227.
11. Gale MJ Jr, Korth MJ, Katze MG. Repression of the PKR protein kinase by the hepatitis C virus NS5A protein: a potential mechanism of interferon resistance. Clin Diagn Virol 1998;10:157-162.
12. Nousbaum J, Polyak SJ, Ray SC, Sullivan DG, Larson AM, Carithers RL, Jr, Gretch DR. Prospective characterization of full-length hepatitis C virus NS5A quasispecies during induction and combination antiviral therapy. J Virol 2000;74:9028-9038.
13. Duverlie G, Khorsi H, Castelain S, Jaillon O, Izopet J, Lunel F, et al. Sequence analysis of the NS5A protein of European hepatitis C virus 1b isolates and relation to interferon sensitivity. J Gen Virol 1998;79 (Pt 6):1373-1381.
14. Layden-Almer JE, Kuiken C, Ribeiro RM, Kunstman KJ, Perelson AS, Layden TJ, Wolinsky SM. Hepatitis C virus genotype 1a NS5A pretreatment sequence variation and viral kinetics in African American and white patients. J Infect Dis 2005;192:1078-1087.
15. Vuillermoz I, Khattab E, Sablon E, Ottevaere I, Durantel D, Vieux C, et al. Genetic variability of hepatitis C virus in chronically infected patients with viral breakthrough during interferon-ribavirin therapy. J Med Virol 2004; 74:41-53.
16. Puig-Basagoiti F, Forns X, Furcic I, Ampurdanes S, Gimenez-Barcons M, Franco S, et al. Dynamics of hepatitis C virus NS5A quasispecies during interferon and ribavirin therapy in responder and non-responder patients with genotype 1b chronic hepatitis C. J Gen Virol 2005;86:1067-1075.
17. Sarrazin C, Herrmann E, Bruch K, Zeuzem S. Hepatitis C virus nonstructural 5A protein and interferon resistance: a new model for testing the reliability of mutational analyses. J Virol 2002;76:11079-11090.
18. Murphy MD, Rosen HR, Marousek GI, Chou S. Analysis of sequence configurations of the ISDR, PKR-binding domain, and V3 region as predictors of response to induction interferon-alpha and ribavirin therapy in chronic hepatitis C infection. Dig Dis Sci 2002;47:1195-1205.
19. Veillon P, Payan C, Le Guillou-Guillemette H, Gaudy C, Lunel F. Quasispecies evolution in NS5A region of hepatitis C virus genotype 1b during interferon or combined interferon-ribavirin therapy. World J Gastroenterol 2007;13:1195-1203.

20. Wohnsland A, Hofmann WP, Sarrazin C. Viral determinants of resistance to treatment in patients with hepatitis C. Clin Microbiol Rev 2007;20:23-38.
21. El-Shamy A, Sasayama M, Nagano-Fujii M, Sasase N, Imoto S, Kim SR, et al. Prediction of efficient virological response to pegylated interferon/ribavirin combination therapy by NS5A sequences of hepatitis c virus and anti-NS5A antibodies in pre-treatment sera. Microbiol Immunol 2007;51:471-482.
22. Okamoto H, Sugiyama Y, Okada S, Kurai K, Akahane Y, Sugai Y, et al. Typing hepatitis C virus by polymerase chain reaction with type-specific primers: application to clinical surveys and tracing infectious sources. J Gen Virol 1992;73(Pt 3):673-679.
23. Lusida MI, Nagano-Fujii M, Nidom CA, Soetjipto, Handajani R, Fujita T, et al. Correlation between mutations in the interferon sensitivity-determining region of NS5A protein and viral load of hepatitis C virus subtypes 1b, 1c, and 2a. J Clin Microbiol 2001;39:3858-3864.
24. Kato N, Hijikata M, Ootsuyama Y, Nakagawa M, Ohkoshi S, Sugimura T, et al. Molecular cloning of the human hepatitis C virus genome from Japanese patients with non-A, non-B hepatitis. Proc Natl Acad Sci U S A 1990;87:9524-9528.
25. Lukasiewicz E, Hellstrand K, Westin J, Ferrari C, Neumann AU, Pawlotsky JM, et al. Predicting treatment outcome following 24 weeks peginterferon alpha-2a/ribavirin therapy in patients infected with HCV genotype 1: utility of HCV-RNA at day 0, day 22, day 29, and week 6. HEPATOLOGY 2007;45:258-259.
26. Jensen DM, Morgan TR, Marcellin P, Pockros PJ, Reddy KR, Hadziyannis SJ, et al. Early identification of HCV genotype 1 patients responding to 24 weeks peginterferon alpha-2a (40 kd)/ribavirin therapy. HEPATOLOGY 2006;43:954-960.
27. Maynard M, Pradat P, Berthillon P, Picchio G, Voirin N, Martinot M, et al. Clinical relevance of total HCV core antigen testing for hepatitis C monitoring and for predicting patients' response to therapy. J Viral Hepat 2003;10:318-323.
28. Bouvier-Alias M, Patel K, Dahari H, Beaucourt S, Larderie P, Blatt L, et al. Clinical utility of total HCV core antigen quantification: a new indirect marker of HCV replication. HEPATOLOGY 2002;36:211-218.
29. Veillon P, Payan C, Picchio G, Maniez-Montreuil M, Guntz P, Lunel F. Comparative evaluation of the total hepatitis C virus core antigen, branched-DNA, and amplicor monitor assays in determining viremia for patients with chronic hepatitis C during interferon plus ribavirin combination therapy. J Clin Microbiol 2003;41:3212-3220.
30. Neumann-Haefelin C, Killinger T, Timm J, Southwood S, McKinney D, Blum HE, et al. Absence of viral escape within a frequently recognized HLA-A26-restricted CD8+ T-cell epitope targeting the functionally constrained hepatitis C virus NS5A/5B cleavage site. J Gen Virol 2007;88:1986-1991.

JOURNAL OF VIROLOGY, Oct. 2009, p. 9993–10006 Vol. 83, No. 19
0022-538X/09/$08.00+0 doi:10.1128/JVI.00509-09

The Hepatitis C Virus Core Protein Contains a BH3 Domain That Regulates Apoptosis through Specific Interaction with Human Mcl-1▽†

Nur Khairiah Mohd-Ismail,[1,2] Lin Deng,[3] Sunil Kumar Sukumaran,[4] Victor C. Yu,[4,5] Hak Hotta,[3] and Yee-Joo Tan[1]*

Collaborative Anti-Viral Research Group, Institute of Molecular and Cell Biology, Singapore[1]; NUS Graduate School for Integrative Sciences and Engineering, Singapore[2]; Division of Microbiology, Kobe University Graduate School of Medicine, Kobe, Japan[3]; Mechanisms of Apoptosis in Mammalian Cell Group, Institute of Molecular and Cell Biology, Singapore[4]; and Department of Pharmacy, Faculty of Science, National University of Singapore, Singapore[5]

Received 11 March 2009/Accepted 8 July 2009

The hepatitis C virus (HCV) core protein is known to modulate apoptosis and contribute to viral replication and pathogenesis. In this study, we have identified a Bcl-2 homology 3 (BH3) domain in the core protein that is essential for its proapoptotic property. Coimmunoprecipitation experiments showed that the core protein interacts specifically with the human myeloid cell factor 1 (Mcl-1), a prosurvival member of the Bcl-2 family, but not with other prosurvival members (Bcl-X_L and Bcl-w). Moreover, the overexpression of Mcl-1 protects against core-induced apoptosis. By using peptide mimetics, core was found to release cytochrome *c* from isolated mitochondria when complemented with Bad. Thus, core is a bona fide BH3-only protein having properties similar to those of Noxa, a BH3-only member of the Bcl-2 family that binds preferentially to Mcl-1. There are three critical hydrophobic residues in the BH3 domain of the core protein, and they are essential for the proapoptotic property of the core protein. Furthermore, the genotype 1b core protein is more effective than the genotype 2a core protein in inducing apoptosis due to a single-amino-acid difference at one of these hydrophobic residues (residue 119). Replacing this residue in the J6/JFH-1 infectious clone (genotype 2a) with the corresponding amino acid in the genotype 1b core protein produced a mutant virus, J6/JFH-1(V119L), which induced significantly higher levels of apoptosis in the infected cells than the parental J6/JFH-1 virus. Furthermore, the core protein of J6/JFH-1(V119L), but not that of J6/JFH-1, interacted with Mcl-1 in virus-infected cells. Taken together, the core protein is a novel BH3-only viral homologue that contributes to the induction of apoptosis during HCV infection.

Hepatitis C virus (HCV), a positive-stranded RNA virus of the family *Flaviviridae*, is the major cause of non-A, non-B hepatitis worldwide. The HCV genome encodes a precursor polyprotein of ~3,000 amino acids (aa) that is processed cotranslationally and posttranslationally to give rise to viral structural and nonstructural proteins (2). The core protein is encoded by the N-terminal portion of the HCV precursor polyprotein and cleaved from the polyprotein by cellular signal peptidase to give the immature form of the core protein (aa 1 to 191). This then is further cleaved by membrane-associated signal peptide peptidase to give the mature core protein, whose C terminus is not precisely known but lies between residues 170 and 179 (see reviews in references 33, 42, and 52). The mature core protein is thought to constitute the HCV capsid and is the predominant form detected in virus particles purified from the sera of patients with chronic HCV infection (42, 74). A recent paper also reported that the maturation of the core protein is required for the production of HCV using the JFH-1 infectious clone (65).

Besides its role in the encapsidation of viral RNA, the core protein has been found to interfere with many cellular pathways, including cell signaling, transcriptional activation, lipid metabolism, carcinogenesis, and apoptosis (see reviews in references 33, 42, and 52). As the regulation of apoptosis during viral infection is an important determinant in the struggle between virus and host for survival, many viruses encode viral proteins that can regulate apoptosis in the infected host cells and manipulate this process to their advantage. In the case of HCV, the mechanisms by which the virus maintains viral persistence and promotes hepatocellular carcinoma are not well understood, but several HCV proteins have the ability to modulate apoptosis (see recent reviews in references 20 and 28). In particular, the core protein has been shown to modulate apoptosis, and it seems that the core protein can inhibit as well as promote apoptosis, depending on the death stimuli and types of cells used (3, 9, 13, 25, 36, 40, 49, 53, 54, 57, 60, 76).

In this study, we characterized one of the mechanisms by which the mature form of the core protein from a genotype 1b strain induces apoptosis in Huh7 cells. Following the experimental designs used in previous studies (29, 38, 40, 55, 72), the mature form of the core protein is assumed to be constituted by residues 1 to 173 of the HCV precursor polyprotein, and

* Corresponding author. Mailing address: Cancer and Developmental Cell Biology Division, Institute of Molecular and Cell Biology, 61 Biopolis Drive, A*STAR (Agency for Science, Technology and Research), Biopolis, Singapore 136873, Singapore. Phone: 65-65869625. Fax: 65-67791117. E-mail: mcbtanyj@imcb.a-star.edu.sg.

† Supplemental material for this article may be found at http://jvi.asm.org/.

▽ Published ahead of print on 15 July 2009.

this shall be referred to as the core protein in this study. Here, we demonstrate that the core protein contains a functional Bcl-2 homology 3 (BH3) domain that is essential for its proapoptotic property and ability to interact with human myeloid cell factor 1 (Mcl-1), a prosurvival member of the Bcl-2 family (31). Detailed molecular analysis and infection studies using the J6/JFH-1 infectious clone showed that the core protein is a bona fide BH3-only protein that contributes to the induction of apoptosis during HCV infection by mimicking Noxa and interfering with the prosurvival function of Mcl-1.

MATERIALS AND METHODS

Construction of plasmids. Expression plasmids for the wild-type core protein and mutants were generated by PCR using Titanium *Taq* DNA polymerase (Clontech Laboratories Inc., Palo Alto, CA). Two plasmids containing full-length HCV genomes were used as templates. The first one is a 1b strain cloned in Singapore (59), and the second is the JFH-1 clone, which is a 2a strain (68). All sequences were confirmed by sequencing performed by the core facilities at the Institute of Molecular and Cell Biology, Singapore. The pXJ40flag vector is used so that a flag epitope is fused to the N terminus of the core protein, and this allows the comparison of protein expression levels with an anti-flag antibody.

Transient transfections, CaspACE fluorometric assay, and Western blot analysis. Transient transfections of Huh7 cells were performed using Lipofectamine reagent (Invitrogen, Carlsbad, CA) according to the manufacturer's protocol. Approximately 16 h after transfection, the activation of caspase-3 was quantified by using a CaspACE fluorometric assay system from Promega Corporation (Madison, WI) as previously described (63).

Western blot analysis was performed as previously described (64). The primary antibodies (anti-myc monoclonal and anti-myc and anti-Mcl-1 polyclonal [Santa Cruz Biotechnology, Santa Cruz, CA], anti-Mcl-1 monoclonal [Calbiochem, La Jolla, CA], anti-actin monoclonal, anti-Hsp-60 monoclonal, anti-flag monoclonal and polyclonal [Sigma, St. Louis, MO], anti-poly[ADP-ribose] polymerase [PARP] polyclonal [Cell Signaling Technology Inc., Beverly, MA], anti-cytochrome *c* monoclonal [BD PharMingen, BD Biosciences, San Jose, CA], and anti-Noxa [Imgenex, San Diego, CA]) were purchased. Anti-core protein monoclonal antibody (clone 2H9; a kind gift from T. Wakita, Department of Virology II, National Institute of Infectious Diseases, Tokyo, Japan) was used to detect the core protein of HCV (68).

Coimmunoprecipitation experiments. For the coimmunoprecipitation experiments, each 6-cm dish of cells was resuspended in 200 μl of immunoprecipitation (IP) buffer (50 mM Tris-HCl, pH 8, 150 mM NaCl, 0.5% NP-40, 0.5% deoxycholic acid, 0.005% sodium dodecyl sulfate [SDS], and 1 mM phenylmethylsulfonyl fluoride) and subjected to freeze-thawing six times. Anti-flag monoclonal antibody conjugated to Sepharose beads (Sigma) were added to 150 μl of the lysates, and the mixture was subjected to end-over-end mixing at 4°C for 6 h. Beads were washed four times with cold IP buffer, and then 15 μl of Laemmli's SDS buffer was added and the samples were boiled at 100°C for 5 min to release the immunocomplexes. Samples were separated by SDS-polyacrylamide gel electrophoresis and subjected to Western blot analysis.

Alternatively, rabbit anti-Mcl-1 polyclonal antibody was used to immunoprecipitate endogenous Mcl-1 protein. In this case, 7 μg of antibody (either anti-Mcl-1 or anti-hemagglutinin [HA] polyclonal antibody [Santa Cruz Biotechnology]) was added to the lysates obtained from two dishes of cells and allowed to mix for 1 h at room temperature. Protein A agarose beads (Roche, Indianapolis, IN) were added, and the mixture was subjected to end-over-end mixing at 4°C overnight. The coimmunoprecipitated proteins then were detected as described above.

Quantification of autoradiographs. An imaging densitometer (Bio-Rad, Hercules, CA) was used for the quantification of the intensities of specific bands on autoradiographs.

In vitro cytochrome *c* release assay. For the in vitro cytochrome *c* release assays, mitochondria were isolated from 293T cells as previously described (22). Briefly, 293T cells were suspended in isolation buffer (320 mM sucrose, 1 mM EDTA, 50 mM HEPES [pH 7.5]) and disrupted by 25 expulsions through a 27-gauge needle. The disrupted cells were spun at 1,000 × *g* for 10 min to remove cell debris and nuclei. The supernatant was centrifuged at 7,000 × *g* for 10 min, and the pellet was retained as the heavy membrane fraction containing the mitochondria. The mitochondrion-containing pellets then were resuspended in assay buffer (250 mM sucrose, 2 mM KH_2PO_4, 5 mM sodium succinate, 25 mM EGTA, and 10 mM HEPES [pH 7.5]) at 0.5 mg/ml. Equal amounts of mitochondria were treated with the indicated peptides for 30 min at room temperature, followed by centrifugation. Both the supernatant and pellet then were subjected to SDS-polyacrylamide gel electrophoresis, followed by Western blot analysis to determine the amount of cytochrome *c* released from the mitochondria. Hsp-60 was used as a loading control for the pellet.

Synthesis of peptides. A peptide that corresponds to residues 118 to 149 of the genotype 1b core protein (NLGKVIDTLTCGFADLMGYIPLVGAPLGG AAR) was synthesized and purified to 95% purity (Sigma Genosys, Japan). Peptides containing the BH3 domain of Bad (NLWAAQRYGRELRRMSDEF VDSFKK) or Noxa (VPADLKDECAQLRRIGDKVNLRQKL) also were synthesized and purified to 95% purity (Mimotopes, Clayton, Victoria, Australia).

Generation of recombinant HCV. The pFL-J6/JFH-1 plasmid encoding the entire viral genome of a chimeric strain of HCV genotype 2a, J6/JFH-1 (37), was kindly provided by C. M. Rice, Center for the Study of Hepatitis C, The Rockefeller University. To generate mutant virus possessing a core protein mutation, a nucleotide substitution was introduced into pFL-J6/JFH-1 by site-directed mutagenesis using a QuikChange site-directed mutagenesis kit (Stratagene, La Jolla, CA). All PCR-amplified DNA fragments were verified extensively using an ABI PRISM 3100-Avant Genetic Analyzer (Applied Biosystems, Foster City, CA). Each of the plasmids was linearized by XbaI digestion and in vitro transcribed by using T7 RiboMAX (Promega) to generate the full-length viral genomic RNA. The in vitro-transcribed RNA (10 μg) was transfected into Huh7.5 cells by means of electroporation (975 μF, 270 V) using a Gene Pulser (Bio-Rad). The cells then were cultured in complete medium, and the supernatant was propagated as a virus stock. Culture supernatants of uninfected cells served as a control (mock preparation). Virus infectivity was measured by indirect immunofluorescence as previously described (17) and expressed as cell-infecting units (CIU) per milliliter.

Proliferation, caspase-3, and DNA fragmentation assays. Huh7.5 cells were seeded in 96-well plates at a density of 1.0×10^4 cells per well and cultured overnight. The cells then were infected with recombinant HCV at a multiplicity of infection of 0.1 CIU/cell or with a mock preparation. At different time points postinfection (p.i.), cell viabilities were determined by WST-1 proliferation assays (Roche, Mannheim, Germany) as described previously (17, 48).

Caspase-3 and DNA fragmentation assays also were performed on the infected cells as previously described (17).

HCV RNA quantitation. To measure intracellular HCV RNA replication levels, total RNA was extracted from the cells using an RNeasy Mini kit (Qiagen, Valencia, CA) according to the manufacturer's instructions. One microgram of total RNA was reverse transcribed using a QuantiTect reverse transcription kit (Qiagen) with random primers and was subjected to quantitative real-time PCR analysis using SYBR premix Ex *Taq* (Takara Bio, Kyoto, Japan) in a MicroAmp 96-well reaction plate and an ABI PRISM 7000 (Applied Biosystems, Foster, CA). The primers used to amplify an NS5A region of the HCV genome were 5′-AGACGTATTGAGGTCCATGC-3′ (sense) and 5′-CCGCAGCGACGGTG CTGATAG-3′ (antisense). As an internal control, human glyceraldehyde-3-phosphate dehydrogenase expression levels were measured using primers 5′-G CCATCAATGACCCCTTCATT-3′ (sense) and 5′-TCTCGCTCCTGGAAGA TGG-3′ (antisense).

Statistical analysis. Either the two-tailed Student's *t* test or one-way analysis of variance (using SPSS version 16.0) was applied to evaluate the statistical significance of differences measured from the data sets. $P < 0.05$ was considered statistically significant.

RESULTS

A BH3-like domain is present in the core protein. The family of Bcl-2 proteins constitutes one of the biologically important gene products in the regulation of apoptosis (see recent reviews in references 1, 16, 67, and 75). The Bcl-2 proteins may be classified broadly into three classes: prosurvival members containing multiple Bcl-2 homology domains, proapoptotic members containing multiple Bcl-2 homology domains, and proapoptotic members containing the BH3 domain only. The examination of the amino acid sequence of the core protein revealed that there is a BH3-like domain near the C terminus. An alignment of this domain with BH3 domains of the Bcl-2 family of proteins is shown in Fig. 1A. The BH3-like domain of the core protein contains L (residue 119) and D (residue 124)

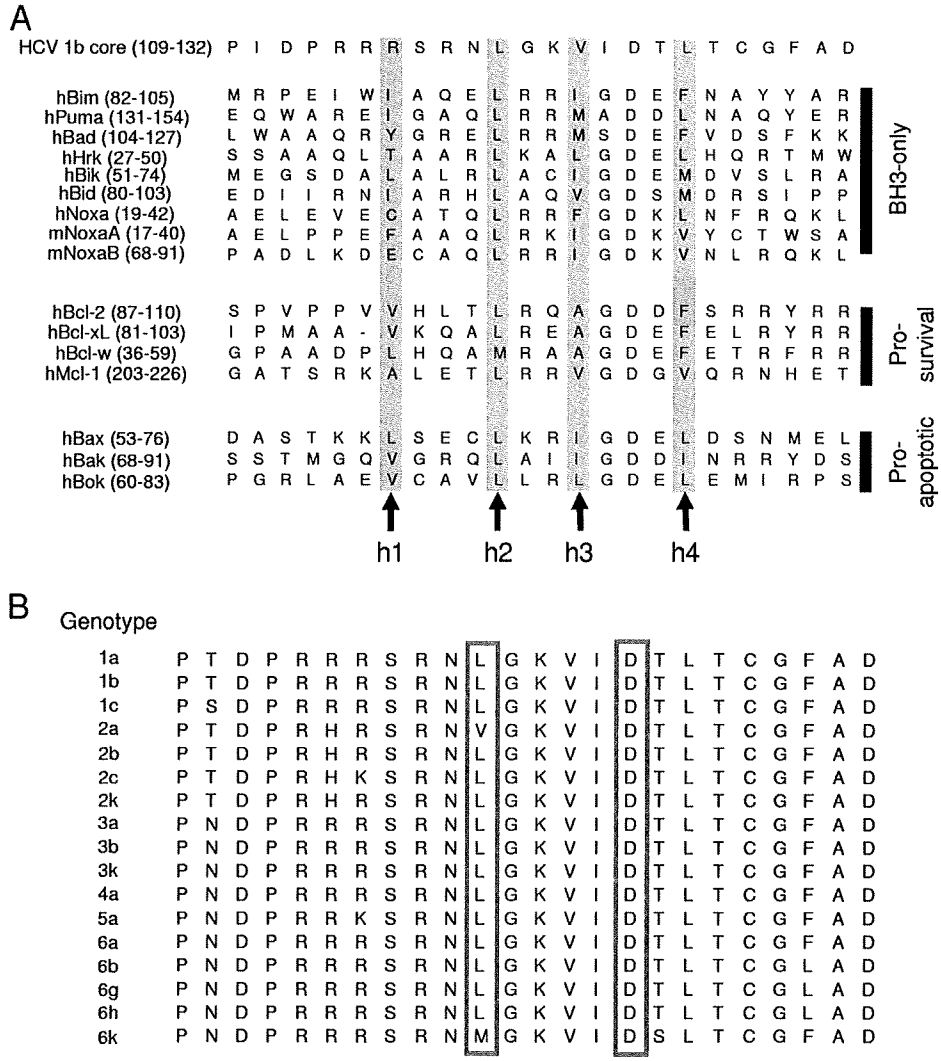

FIG. 1. Identification of a BH3-like domain in the core protein. (A) Alignment of the BH3 domain of the genotype 1b core protein with the BH3 domains of members of the Bcl-2 family. Numbers in parentheses represent the positions of amino acid residues of the respective proteins. The four hydrophobic amino acids that make critical contacts with residues in the BH3 recognition grooves present on the surfaces of the prosurvival Bcl-2 family proteins are indicated as h1 to h4. (B) Alignment of the core protein (residues 109 to 132) of different genotypes. The consensus sequences for these genotypes were obtained from http://hcv.lanl.gov/content/hcv-index. The highly conserved L and D residues, at positions 119 and 124 of the genotype 1b core protein, respectively, in BH3 domains are boxed.

separated by four residues, as in other known BH3 domains. This domain is highly conserved among the major HCV genotypes, with the exception of genotypes 2a and 6k, which have V and M residues at position 119, respectively (Fig. 1B).

The BH3 domain of the core protein is essential for the induction of apoptosis and its interaction with human Mcl-1. The overexpression of the core protein (with a flag epitope at the N terminus) in Huh7 cells, via the transient transfection of a cDNA expression plasmid containing the genotype 1b core protein gene, induced significant levels of apoptosis as determined by the activation of caspase-3, which is a hallmark of apoptosis (Fig. 2A). The deletion of the BH3 domain in the core protein (designated coreΔ115-128aa) abolished its proapoptotic property, indicating that this domain is essential for the induction of apoptosis. Consistently, the cleavage of endogenous PARP, a substrate of activated caspase-3, was clearly observed in Huh7 cells expressing the wild-type core protein but not in those expressing coreΔ115-128aa (Fig. 2B).

To understand how the core protein modulates the function of the Bcl-2 family of proteins, coimmunoprecipitation experiments were performed to determine if the core protein can interact with representative prosurvival members of the Bcl-2 family. As shown in the top panel of Fig. 3A, Mcl-1 was specifically coimmunoprecipitated by the core protein (lane 8) but not by an irrelevant protein, glutathione *S*-transferase (GST) (lane 7). The BH3 domain of the core protein is essential for its interaction with Mcl-1, as coreΔ115-128aa failed to coimmunoprecipitate Mcl-1 (lane 9). These results indicate that the core protein induces apoptosis by interfering directly with the prosurvival function of Mcl-1. In contrast, no significant inter-

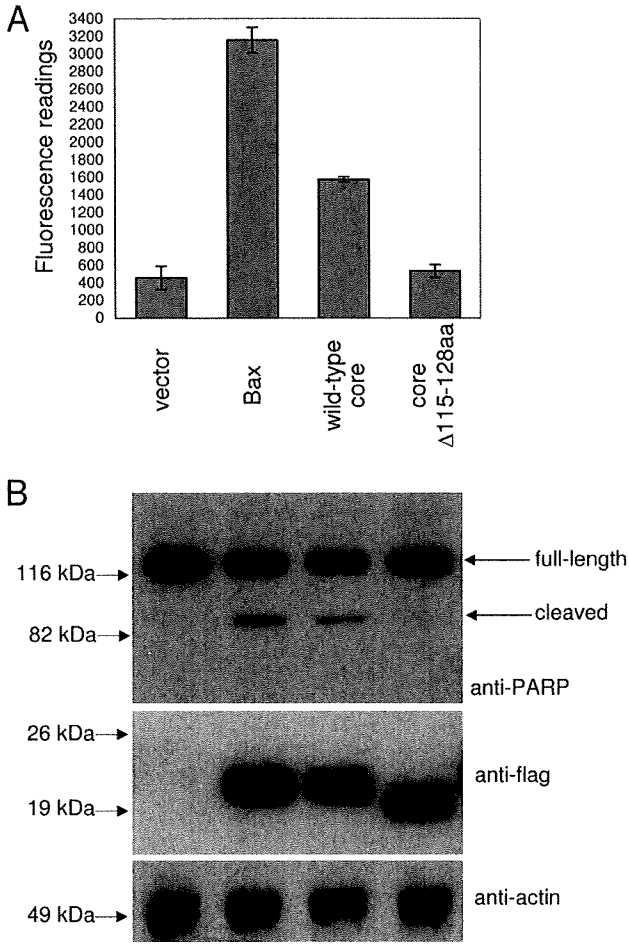

FIG. 2. Induction of apoptosis by the overexpression of the core protein in Huh7 cells. (A) A CaspACE fluorometric assay system from Promega Corporation (Madison, WI) was used to measure the activation of caspase-3, which is a hallmark of apoptosis, in Huh7 cells that were transfected with vector only, a classical apoptosis inducer (Bax), the wild-type core protein, and a core protein mutant lacking the putative BH3 domain (coreΔ115-128aa). All experiments were performed in triplicate, and the average values with standard deviations are plotted. (B) Western blot analysis also was performed to determine the cleavage of endogenous PARP, which is a substrate of activated caspase-3, from 116 to 83 kDa (top). Similarly, the expression levels of the different proteins were determined using anti-flag antibody (middle). The amounts of total cell lysates loaded were verified by measuring the levels of endogenous actin (bottom).

action was observed between the core protein and two other prosurvival proteins, Bcl-X_L and Bcl-w (lanes 1 to 6).

The interaction between the core protein and endogenous Mcl-1 was determined by overexpressing the core protein in Huh7 cells. As shown in Fig. 3B, the core protein was coimmunoprecipitated with endogenous Mcl-1 (lane 3). On the other hand, the core protein was not coimmunoprecipitated when an irrelevant antibody (anti-HA) (lane 4) was used for IP. Consistently with the results in Fig. 3A, only a small amount of coreΔ115-128aa was coimmunoprecipitated with endogenous Mcl-1 (lane 5). To estimate the degree of reduction in the binding of coreΔ115-128aa to endogenous Mcl-1, an imaging densitometer was used to quantify the intensities of specific bands on the autoradiographs obtained in three independent coimmunoprecipitation experiments (see Fig. S1 in the supplemental material). The ratios of signals for the expression of flag-tagged core protein, endogenous Mcl-1, and actin (internal control) all are close to 1 (0.94 to 1.14), indicating that the expression levels of these proteins in the two sets of cells (either transfected with cDNA construct for expressing flag-core or flag-coreΔ115-128aa) were similar. From the three independent experiments, the average amount of coreΔ115-128aa coimmunoprecipitated specifically by the Mcl-1 antibody is 14.2% (± 10.7%) of the amount of wild-type core protein coimmunoprecipitated. This implies that the deletion of the BH3 domain does not completely abolish the interaction between the core protein and endogenous Mcl-1 but reduces the interaction greatly.

Overexpression of Mcl-1 or Bcl-X_L prevents core protein-induced apoptosis. To examine the protective effects of the prosurvival Bcl-2 proteins in Huh7 cells, transfections were performed with plasmids expressing myc-tagged Bcl-2, Bcl-X_L, Bcl-w, or Mcl-1 (Fig. 4A and B). Consistent with studies of other cell lines (12, 66), the transient high-level expression of Bcl-2 also caused apoptosis in Huh7 cells (lane 1). Interestingly, the overexpression of Bcl-w also induced a significant level of apoptosis in Huh7 cells (lane 3), and this phenomenon has not been reported previously. Cells overexpressing Bcl-X_L, but not Mcl-1, also had a slightly higher level of apoptosis than that of the vector control cells (lanes 2 and 4).

Huh7 cells were cotransfected with plasmids for expressing myc-Mcl-1 and flag-core or myc-Bcl-X_L and flag-core. As shown in Fig. 4C and D, the level of apoptosis was significantly reduced in cells expressing both Mcl-1 and the core protein (lane 3) compared to those expressing the core protein only (lane 2). When the same experiment was repeated using Bcl-X_L, the level of apoptosis was reduced to a lesser extent (lane 5). However, this may be due to the low level of apoptosis induced by the overexpression of Bcl-X_L (lane 6). The level of the core protein expressed in the presence of Bcl-X_L also was decreased greatly, but the smaller amount of the core protein expressed still induced a high level of apoptosis (lane 5). However, when a broad caspase inhibitor (z-VAD-fmk) was used, the core protein level in cells coexpressing Bcl-X_L increased (see Fig. S2 in the supplemental material), indicating that the transfection efficiencies were similar in the different samples. To resolve this uncertainty, the experiment was repeated with a smaller amount of Bcl-X_L plasmid (0.5 μg). Under this condition, the overexpression of Bcl-X_L did not induce apoptosis (lane 8), and the level of apoptosis also was reduced in cells expressing both Bcl-X_L and the core protein (lane 7) compared to those expressing the core protein only (lane 2). Thus, the results show that the overexpression of either Mcl-1 or Bcl-X_L protects against core protein-induced apoptosis.

Bad enhances the ability of the core protein to release cytochrome *c* from isolated mitochondria. The ability of a core protein peptide, which contains residues 118 to 149 of the genotype 1b core protein, to release cytochrome *c* from the mitochondria was tested using 293T cells instead of Huh7 cells, as the method for the isolation of mitochondria from 293T cells is well established. The core protein induced apoptosis in 293T cells in the same manner as that in Huh7 cells (see Fig.

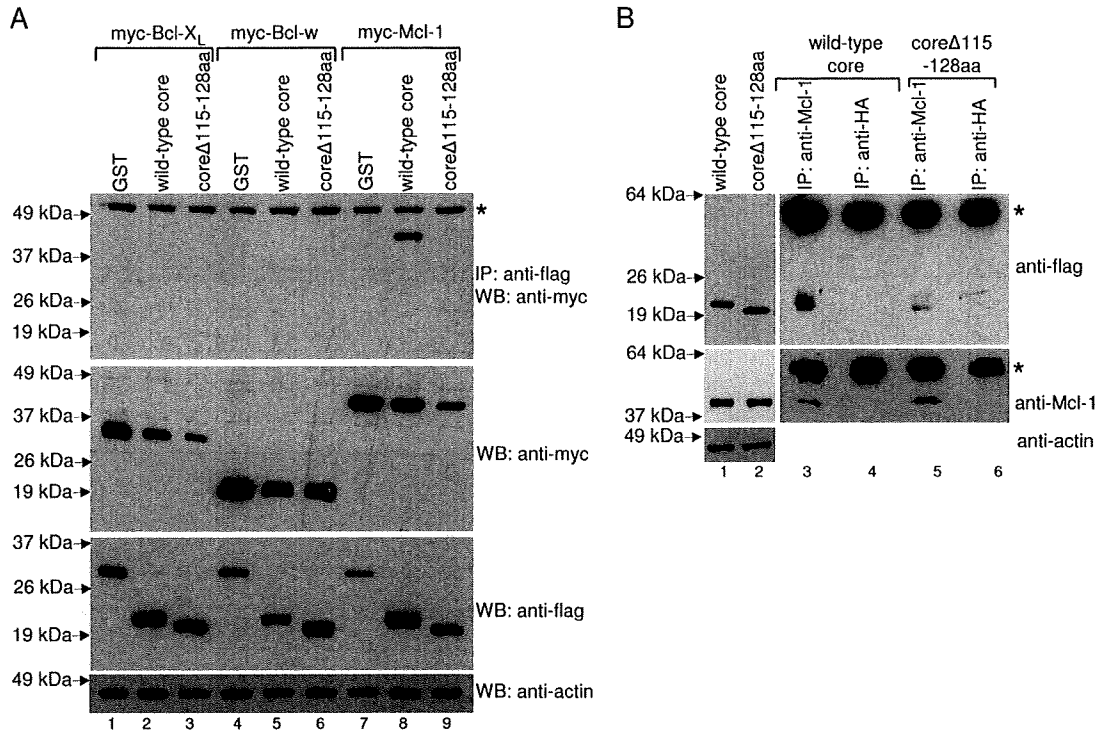

FIG. 3. Interaction of the core protein with prosurvival members of the Bcl-2 family determined by coimmunoprecipitation experiments. (A) Huh7 cells were transfected with cDNA constructs for expressing flag-GST (negative control), flag-core, or flag-coreΔ115-128aa, and myc-tagged prosurvival members of the Bcl-2 family (myc-Bcl-X_L [lanes 1 to 3], myc-Bcl-w [lanes 4 to 6], and myc-Mcl-1 [lanes 7 to 9]). The cells were harvested at ~16 h posttransfection, lysed, and subjected to IP with anti-flag monoclonal antibody conjugated to Sepharose beads. The amount of myc-tagged proteins that coimmunoprecipitated (IP) with the flag-tagged proteins was determined by Western blot analysis (WB) with an anti-myc rabbit polyclonal antibody (top). The amounts of myc-tagged and flag-tagged proteins in the lysates before IP were determined by subjecting aliquots of the lysates to Western blot analysis (middle). The protein marked with an asterisk represents the heavy chain of the antibody used for IP (top), and the amounts of total cell lysates loaded were verified by measuring the levels of endogenous actin (bottom). (B) Huh7 cells were transfected with cDNA constructs for expressing flag-core or flag-coreΔ115-128aa. IP then was performed using anti-Mcl-1 or anti-HA rabbit polyclonal antibodies and protein A agarose beads. The amounts of flag-tagged core protein in the lysates before IP (lanes 1 and 2) or coimmunoprecipitated (lanes 3 to 6) were determined by Western blot analysis with an anti-flag monoclonal antibody (top). Similarly, the amounts of endogenous Mcl-1 in these samples were detected using an anti-Mcl-1 monoclonal antibody (middle). The protein marked with an asterisk represents the heavy chain of the antibody used for IP (top), and the amounts of total cell lysates loaded were verified by measuring the levels of endogenous actin (bottom).

S3 in the supplemental material). As shown in Fig. 5A, both the Bad and core protein peptides were inefficient in inducing the release of cytochrome *c*, as only a small amount of cytochrome *c* was detected in the supernatant from the treated mitochondria when 200 μM of either peptide was used. However, when Bad and core protein peptides were used in combination, the release of cytochrome *c* was observed at the much lower concentration of 50 μM (consisting of 25 μM Bad peptide and 25 μM core protein peptide). Furthermore, the release of cytochrome *c* increased in a dose-dependent manner. The amount of cytochrome *c* left in the treated mitochondria (i.e., pellet) decreased correspondingly, while the amount of control protein, Hsp-60, was not affected.

The same experiment was repeated using the Noxa peptide (Fig. 5B). Consistently with a previous study (11), the Noxa peptide alone was inefficient in inducing the release of cytochrome *c*, but when it was combined with the Bad peptide, the release was significantly enhanced. The peptide(s) dosage required was similar to the amount required for the core protein and Bad, indicating that the complementation between the core protein and Bad is similar to the complementation between Noxa and Bad. In addition, complementation between the core protein and Bad also was observed when they were coexpressed in Huh7 cells (see Fig. S4 in the supplemental material).

The three hydrophobic residues in the BH3 domain of the core protein are important for apoptosis induction. Site-directed mutagenesis and structural studies of the interactions between the prosurvival Bcl-2 proteins and BH3 domains have revealed the mechanism by which BH3 domains are bound to the hydrophobic grooves present on the surfaces of the prosurvival Bcl-2 proteins (see reviews in references 50 and 69). In particular, the BH3 domain usually contains four hydrophobic residues (h1, h2, h3, and h4) (Fig. 1A) that make contacts critical for the stability of the complex. Interestingly, the core protein contains hydrophobic residues at the h2, h3, and h4 positions (Fig. 1A). An alanine substitution experiment was performed to determine if these residues are essential for the proapoptotic property of the core protein (Fig. 6A and B). The results showed that replacement of either L119, V122, or L126